

UNCLASSIFIED

DTRA-TR-99-47

Development of an Infrasound Propagation Modeling Tool Kit

Robert Gibson
David Norris

Report Number ASCO 1999 005

Contract DSWA 01-97-C-0160

October 1999

Prepared by: BBN Technologies
1300 North 17th Street, Suite 1200
Arlington, VA 22209

Prepared for: Defense Threat Reduction Agency
8725 John J. Kingman Road, MS 6201
Fort Belvoir, VA 22060-6201

UNCLASSIFIED

Preface

Many people have assisted the authors in this effort, both through general discussions and by providing several of the base modeling capabilities contained in the InfraMAP software. In particular,

- Rod Whitaker of Los Alamos National Laboratory (LANL) has provided many hours of discussion and direction on the modeling techniques and provided the WKB version of the normal mode code.
- Dean Clauter and Bob Blandford of the Air Force Technical Applications Center (AFTAC) provided guidance regarding the desired capabilities of the software and also provided historical data for validation purposes.
- Doug Drob of NRL's Upper Atmospheric Physics Branch provided advice and assistance regarding use of the HWM and MSISE atmospheric models, available from the NRL web site, and also provided valuable insight regarding approaches to perturbation modeling of the propagation environment.
- Tom Georges of NOAA's Environmental Technology Laboratory provided the HARPA ray tracing code, available from the NOAA/ETL ftp site, and a copy of the software documentation.

Ted Farrell of BBN provided expertise based on development of the HydroCAM modeling software and reviewed the technical progress. Rebecca Nadel of BBN made major contributions to the software development and model validation efforts. Eugene Dorfman of BBN reviewed available underwater sound propagation modeling codes and recommended modeling approaches. Robert Bieri of BBN assisted in the integration of HARPA with the environmental models and contributed to model validation efforts.

We also gratefully acknowledge feedback from those who used the beta versions of InfraMAP: Rod Whitaker, Doug ReVelle, and Tom Armstrong of Los Alamos National Laboratory (LANL), and Dean Clauter of the Air Force Technical Applications Center (AFTAC).

Table of Contents

Section	Page
Preface	ii
Figures	v
Tables	vii
1 Summary	1
2 Introduction	2
2.1 Background.....	2
2.2 Purpose.....	2
2.3 Scope.....	3
2.4 Outline.....	4
3 Methods, Assumptions and Procedures.....	5
3.1 Environmental Characterization.....	5
3.2 Propagation Modeling.....	7
3.3 Variability and Network Performance.....	8
3.4 Software Implementation.....	9
4 Results and Discussion.....	11
4.1 InfraMAP Software Tool Kit.....	11
4.2 Environmental Characterization.....	12
4.2.1 Horizontal Wind Model (HWM).....	13
4.2.2 Mass Spectrometer - Incoherent Scatter Radar Atmospheric Model (MSIS).....	13
4.2.3 Additional Environmental Data.....	13
4.3 Propagation Models.....	15
4.3.1 Ray Tracing.....	18
4.3.2 Normal Modes.....	18
4.3.3 Parabolic Equation.....	19
4.4 Network Performance.....	19
4.5 Reports to the Research Community.....	20

Table of Contents (continued)

Section		Page
	4.6 Sensitivity Analyses.....	23
	4.6.1 Diurnal Sensitivity.....	23
	4.6.2 Seasonal Sensitivity.....	27
	4.6.3 Sensitivity to Solar Magnetic Disturbance.....	30
	4.6.4 Sensitivity to Latitude.....	30
	4.7 Validation Studies.....	34
	4.8 Example Application.....	38
	4.8.1 Scenario.....	38
	4.8.2 Signal Velocity.....	40
	4.8.3 Azimuth Deviation.....	41
	4.8.4 Summary of Predicted Biases.....	43
	4.8.5 Effect of Biases on Localization.....	43
5	Conclusions and Recommendations.....	46
6	References.....	48
Appendix		
	Abbreviations and Acronyms.....	A-1
	Distribution List.....	DL-1

Figures

Figure		Page
1	Global display of wind magnitude at fixed altitude (from HWM).....	14
2	Temperature profiles at locations along a path (from MSISE).	15
3	Vertical projection of ray paths (Eigenrays).	16
4	Waveform calculated using normal modes.	17
5	Amplitude field from parabolic equation model.	17
6	Perturbation spectrum.....	21
7	Perturbation profile.....	21
8	Ray ground hit points.	22
9	Probability density estimate.	22
10	Travel time variations over diurnal cycle; 2500 km path.....	25
11	Azimuth deviation variations over diurnal cycle; 2500 km path.	25
12	Zonal wind variations over diurnal cycle; Central Asia (+Eastward).	26
13	Meridional wind variations over diurnal cycle; Central Asia (+Northward).....	26
14	Zonal wind variations over diurnal cycle; Nevada (+Eastward).	27
15	Meridional wind variations over diurnal cycle; Nevada (+Northward).	28
16	Eastward eigenrays from Nevada; Day 301.	28
17	Travel time variations over annual cycle; 1000 km path.	29

Figures (continued)

Figure		Page
18	Travel time variability due to solar magnetic disturbance.	31
19	Azimuth deviation variability due to solar magnetic disturbance.	31
20	Zonal winds (+E) along slice of atmosphere from South Pole to North Pole, 78° E.	32
21	Variability in travel time due to source latitude; meridional path.	33
22	Variability in azimuth deviation due to source latitude; meridional path.	34
23	Modeled eigenrays from El Paso bolide to TXIAR array.	36
24	Modeled eigenrays from El Pasobolide to LANL array.	36
25	Paths from South Pacific source location to nine infrasound stations; 1000 km contours.	39
26.	Zonal winds (+Eastward) at South Pacific source location over annual cycle.	39
27	Signal velocities to 9 IMS stations at a range of azimuths; Day 1.	40
28	Signal velocities to 9 IMS stations at a range of azimuths; Day 128.	41
29	Azimuth deviations to 9 IMS stations at a range of azimuths; Day 1.	42
30	Azimuth deviations to 9 IMS stations at a range of azimuths: Day 182.	42
31	Back-azimuths from 9 IMS stations, with contours at 100 km increments; Day 1.	44
32	Back-azimuths from 9 IMS stations, with contours at 100 km increments; Day 182.	44

Tables

Table		Page
1	Capabilities and characteristics of propagation models.	16
2	Summary of diurnal variability results for four geometries.	24
3	Summary of seasonal variability results for two geometries.	29
4	Comparison of observed and modeled arrivals at TXIAR array.	37
5	Comparison of observed and modeled arrivals at LANL array.	37

Section 1

Summary

The development of technologies for utilizing a network of atmospheric infrasound sensors to monitor compliance with a Comprehensive Nuclear-Test-Ban Treaty (CTBT) is currently underway. Detection and localization capabilities are required for achievement of an effective monitoring system. The dynamic nature of the atmosphere, the uncertainties involved in characterizing high-altitude temperatures and winds, and the long ranges over which infrasound signals propagate combine to make accurate predictions of infrasound propagation difficult. Reliable models are needed in order to predict infrasound propagation paths from potential event locations worldwide. Existing model implementations can be difficult to use and neglect dynamic atmospheric effects.

In this effort, propagation modeling techniques and sources of atmospheric data were reviewed, and models and databases deemed most suitable for application to infrasound monitoring were selected for incorporation in an integrated software tool kit. The software called InfraMAP, for Infrasonic Modeling of Atmospheric Propagation, was developed to support the CTBT researcher and analyst. The software includes three types of high-fidelity propagation models: ray tracing, normal modes, and parabolic equation (PE); it also includes two empirical models of the global atmosphere that include temporal effects: a horizontal wind model, and a temperature/density model. Enhancements to the existing propagation models were also implemented to improve the functionality of the software. Algorithms were developed for assessing variability in propagation parameters, specifically travel time and arrival azimuth, based on perturbations to mean wind profiles.

The propagation models are integrated with the environmental characterizations through a common graphical user interface. The software is user-friendly and provides a wide range of display options for visualizing both the atmospheric models and the results from the propagation models. Following the development of a prototype “beta” version of the software, InfraMAP was installed at two sites, and scientists there were trained on its use. Feedback was obtained from the users, based on their experience with the software and on their requirements, and beta-testing recommendations were incorporated in the final version of the software. A user’s manual for the software was prepared. Progress and results were reported to the research community throughout the effort, in the form of symposium posters, workshop presentations, and technical papers.

Output from the propagation models was compared to measured data from historical events of interest in order to validate the models. These comparisons have allowed identification of both the strengths of the software and areas where future efforts should be focused. The software was used extensively both to model scenarios of interest for CTBT monitoring and also to study the sensitivity of propagation results to variations in the environment, the event time, or the location. Results of the analyses demonstrate the utility and flexibility of the software and also highlight important issues that must be addressed in order to achieve adequate estimates and estimate bounds of infrasound source location.

Section 2 Introduction

2.1 Background.

Verification of the Comprehensive Nuclear-Test-Ban Treaty (CTBT) will require the ability to detect, localize, and discriminate nuclear events on a global scale. Monitoring systems such as the International Monitoring System (IMS) rely on several sensor technologies to perform these functions. The current IMS infrasound system design includes a network of low-frequency atmospheric acoustic sensor arrays, which contribute primarily to the detection and localization of atmospheric nuclear events.

Infrasound source location estimates are made using a “back azimuth” approach that entails looking back along the azimuths measured by two or more arrays. Travel time information can be used to improve the infrasound source location estimates. Because of the temporal and spatial variability of the atmosphere, there are no stable, reliable, simply predictable propagation paths that can be used in standard back-azimuth and time-of-arrival localization approaches.

The technical challenges involved in monitoring the CTBT using infrasound include the proper consideration of the effects of upper atmospheric dynamics on propagation. The large spatial and temporal variability of the atmospheric temperature and wind speed produces a very complicated infrasound propagation environment in which sound speed varies with time, location and altitude. Variability in sound speed and uncertainties inherent in characterizations of temperature and wind represent sources of uncertainty in source localization. The approximations currently in use operationally are expected to result in localization performance significantly worse than the monitoring network design goal of 1000 sq. km [Clauter and Blandford, 1996].

Numerous propagation models have been developed for the study of atmospheric and ocean acoustics. Prior to this effort, the atmospheric models applicable to infrasound were used primarily in basic research, were individually exercised on a case-by-case basis, and were often restricted by assumptions such as range-independence or a windless, constant sound speed. Furthermore, user interface to the models was not straightforward.

Similarly, many databases and models characterizing the atmosphere have been compiled. However, few if any investigations have been conducted of the suitability of the various databases for use in conjunction with long-range infrasound propagation models. No straightforward interface between environmental data and propagation models has existed.

2.2 Purpose.

It has been anticipated that the ability to identify infrasound phases, and to include the appropriate travel-time and bearing corrections for each arrival into localization procedures, would dramatically improve localization performance. Reducing uncertainties in location

estimates from the infrasound network would also improve the ability to associate detected events with hydroacoustic and seismic signals.

The purpose of this effort was to develop a tool that will allow infrasound analysts and researchers to easily model propagation through realistic characterizations of the atmosphere. The tool should provide environmental integration and execution capabilities for a baseline set of acoustic propagation models. Development of such an integrated set of models should allow for high fidelity propagation modeling by offering features such as range-dependent sound speed and winds. The ability to predict the critical infrasound propagation characteristics (travel time, azimuth, amplitude) that affect localization and network performance would therefore be enhanced.

The functionality of the software tool developed during this effort addresses these needs and the problems of interest in CTBT monitoring. The tool allows the research community to model or evaluate the performance of infrasound localization and detection algorithms. Use of the software is anticipated to lead to increased efficiency and effectiveness of CTBT operational and research components.

Once the modeling tool has been developed, systematic sensitivity analyses and validation studies are necessary to understand the effect of environmental and model parameters on accurate modeling of long range infrasound propagation. These investigations serve to identify specific areas where additional infrasound research and further development of modeling capabilities are needed. They will also help to define requirements for an infrasound knowledge database. The CTBT research community will benefit from improved understanding of modeling issues, e.g., confidence bounds on predictions, the need for *in situ* atmospheric data or synoptic models, and the relative importance of temporal and spatial variability in the environment.

2.3 Scope.

The scope of this effort was to develop software that can be easily used to meet infrasound modeling requirements for CTBT monitoring purposes. The specific goals for this effort were:

- Develop an integrated software system capable of:
 - (a) defining the state of the atmosphere, such as temperature and wind speed profiles, as required for infrasound propagation modeling;
 - (b) predicting the phases, velocities, travel times, azimuths and amplitudes of atmospheric explosions measured by infrasound sensors;
 - (c) supporting prediction of localization area of uncertainty and detection performance, by quantifying environmental variability and propagation sensitivity.
- Conduct sensitivity studies to determine the effects of environmental variables on infrasound propagation, and validate that the modeling software techniques are consistent with measured data.
- Prepare a users' manual and documentation describing the models.

Progress toward these goals is discussed in the following sections.

2.4 Outline.

This section provides an introduction to the research effort. The remainder of the report summarized the technical work that has been performed. Section 3 addresses methods, assumptions, and procedures in the model development process. Section 4 discusses the results of the effort by describing the software and its functionality, summarizing studies that have been performed using the software and presenting example applications. The report ends with conclusions and recommendations.

Section 3

Methods, Assumptions and Procedures

This section describes the procedures that were followed during the development and evaluation of the InfraMAP software. First the selection of environmental characterizations is discussed. This is followed by discussions of the selection of propagation models and the approach to network analysis and variability assessment. Finally, the software development methods are summarized.

3.1 Environmental Characterization.

In order to make adequate predictions of infrasound propagation, it is necessary to identify environmental characterizations that are suitable for defining the propagation environment. Determination of the atmospheric sound propagation environment requires knowledge of temperature and wind speed profiles.

The existence of multiple atmospheric layers and large spatial and temporal variability in the atmospheric temperature and wind speed produces a very complicated infrasound propagation environment. Lower, middle and upper atmospheric temperature and wind data, required for predicting infrasound propagation paths, are currently available in a variety of formats at varying temporal and spatial resolutions, but no one data source contains all of the required environmental parameters at all locations and altitudes. Most of the readily accessible data pertains to altitudes less than 30 km, whereas infrasound propagation modeling requires information at much higher altitudes. Multiple atmospheric databases and models have been evaluated for use in InfraMAP, with consideration given to spatial and temporal resolution, coverage, and ease of implementation.

For an integrated infrasound modeling capability, both historical and “real-time” or updated environmental data are potentially useful for determining the best estimate of the environmental conditions affecting infrasound propagation. Consideration of the merits of individual data sources includes:

- Which sources of information have the most complete coverage (location, altitude and time)?
- Are these data at a resolution sufficient for accurate infrasound modeling?
- How should different data sources at different atmospheric layers be joined together?

Data sources generally fall into one of two categories: (1) raw data, such as those from individual measurements, and (2) assimilated data, which may consist of data on a standard grid or models that characterize a set of observed data.

Examples of raw data sources include radiosondes, satellites, and surface weather stations. None of the raw data sources provides the complete set of temperature and wind speed profile

information needed for infrasound modeling. If raw data are used in conjunction with propagation models, temperature and wind speed profiles must be merged and interpolated onto a uniform grid to be supplied as input to the models. There are a number of technical issues that arise when merging databases together, especially when the component databases have different resolutions or coverage. These issues include:

- Accessing data from a variety of formats,
- Interpolation and extrapolation,
- Accounting for the various measurement error bounds, and
- Forming a consistent, useful data representation for processing the data in multiple software applications.

Assimilated data sources are convenient since data quality control, interpolation and extrapolation have been performed by the generating organization. The atmospheric models used in data assimilation generally account for some temporal effects; however, in most instances, their output data represent the best fit to historical measurements rather than predictions based on updated or near-real-time measurements. Therefore, assimilated data sources that are based purely on historical databases will not accurately predict all of the atmospheric fluctuations that may occur on relatively short time scales.

Several assimilated atmospheric databases and software products were obtained from government sources. These include:

- Upper Air Gridded Climatology, (Navy FNMOC);
- Global Upper Air Climatic Atlas, Volumes I and II (Navy FNMOC);
- Marine Climatic Atlas of the World (Navy FNMOC);
- International Station Meteorological Climate Summary, (Navy FNMOC);
- Extreme and Percentile Environmental Reference Tables, (Air Force Combat Climatology Center);
- Upper Air Climatology, (Air Force Combat Climatology Center).

Additional databases from NOAA's National Climatic Data Center (NCDC) and from NASA's Goddard Space Flight Center were also investigated.

Two empirical atmospheric models, developed at NASA and currently maintained by the Naval Research Laboratory, were also obtained. These models were selected for integration with the propagation models in InfraMAP. They are:

- the Horizontal Wind Model (HWM) [Hedin *et al.*, 1996] and
- the Extended Mass Spectrometer - Incoherent Scatter Radar (MSIS or MSISE) temperature and density model [Picone *et al.*, 1997].

HWM provides zonal and meridional wind components, and MSISE provides temperature, density and atmospheric composition. These environmental models have global coverage from the ground into the thermosphere, account for diurnal and annual effects, and were anticipated to

be relatively easy to integrate. The models are described in more detail in Section 4. Historical solar and geomagnetic data that are used as input to the models were obtained from the National Geophysical Data Center (NGDC).

The use of updated data in conjunction with the assimilated databases and empirical models was also investigated. This capability could potentially improve the characterization of the infrasound propagation environment. Some of the issues that must be addressed include:

- Are these data updated at a sufficient rate?
- How should data be accessed?
- Is there reliable global coverage 24 hours a day?
- How should updated raw data be used to supplement an assimilated data set?

A procedure was developed during this effort for downloading and formatting radiosonde data from the National Weather Service web site. A spline technique was used during this effort to join a radiosonde profile to a modeled profile for application to a case of interest. Atmospheric research satellites represent another potential source of updated raw data. However, none of the updated sources of raw data provides the complete set of temperature and wind speed profile information needed for infrasound modeling.

Based on the success of the empirical models at defining the propagation environment in the InfraMAP software, it was determined that the use of updated or *in situ* data sources would not be automated during this effort. Updated environmental profiles, for example radiosonde data, can be used in conjunction with the propagation models, in a range independent mode, via a software option that allows user-defined profiles. The software does, however, provide the infrastructure to incorporate updated atmospheric data in the future, for purposes of improving the estimate of current propagation conditions. For example, the Navy's updated climatological assimilation NOGAPS (Naval Operational Global Atmospheric Prediction System), which uses an extensive data set of ship-based, land-based and satellite measurements to provide gridded wind speed at several altitudes every 12 hours, may be a candidate for integration in future efforts.

3.2 Propagation Modeling.

It was anticipated that a range of modeling capabilities would be required in order to meet the CTBT monitoring objectives of predicting travel time, azimuth, amplitude, and ultimately waveform or spectral characteristics of infrasound phases. A variety of infrasound propagation models exist that can account for varying degrees of lateral and vertical variability in wind and sound speed. However, no one model is sufficient for predicting all essential propagation features. Classes of propagation modeling techniques were evaluated in order to determine their strengths and weaknesses and to identify specific models to be integrated in the software.

Models were evaluated to determine suitability for handling environmental features such as: range-dependence, double-channel sound speed profiles, wind speeds with magnitudes that approach the ambient sound speed, reflections from the earth's surface, etc. For each model, it was necessary to determine whether it would be feasible to integrate range dependent

environmental characteristics or if model execution would be restricted to range independent profiles. Similarly, the feasibility of incorporating absorption into each of the models was addressed; available atmospheric absorption models were reviewed as part of this effort.

Ray theory in a moving inhomogeneous medium is well established and accounts for wind effects in three dimensions. It permits evaluation of the ray trajectories that infrasound waves might follow through laterally varying wind and sound speed profiles. In addition to vertical and horizontal refraction, the model accounts for horizontal translation of the ray path, which can cause significant azimuth biases in the propagation path. An advantage of the ray tracing technique is that it is capable of stepping either forward from a source or backward from a receiver. A ray tracing code developed at NOAA [Jones, *et al.*, 1986] was obtained.

Pierce developed a computer code based on the normal mode theory for infrasound propagation in a relatively low frequency band of interest, motivated by interest in long range propagation of infrasound due to large (i.e., megaton yield) events [Pierce and Kinney, 1976; Pierce *et al.*, 1973; Pierce and Posey, 1970]. The normal mode approach is generally useful for estimating received time series or waveforms. A version of Pierce's normal mode code, modified to determine propagation of higher frequency modes, was provided to BBN by Los Alamos National Laboratory (LANL).

Parabolic equation (PE) models are frequently used in underwater acoustics and in short range atmospheric acoustics. Following an informal literature survey and review of available parabolic equation software, an implementation of the wide-angle finite-difference PE model was developed internally at BBN for use in evaluating infrasound propagation.

Fast field programs (FFP's) are frequently used for modeling windless, short range scenarios. A review was conducted of available software. FFP implementations useful for infrasound studies were concluded to be costly to develop and computationally intensive. Therefore, a FFP capability was not included in the software.

The use of empirically derived relationships to estimate key propagation parameters was evaluated for inclusion in the software. These candidate techniques were considered in order to offer the capability of very rapid "zeroth-order" estimates of travel time, azimuth, and amplitude for a given scenario. Feedback obtained from the research community indicated that efforts in this area should be given a lower priority than efforts in other areas, so these models were not incorporated.

Before software integration of a selected model was undertaken, the model was exercised using simple environmental profiles as test cases. Analytic results from propagation theory were compared to numerically calculated results.

3.3 Variability and Network Performance.

Approaches to assessing localization performance of an infrasound network were reviewed. Goals of a network model include characterization of the Area of Uncertainty, which summarizes the effects of all uncertainties in the localization solution including propagation uncertainties.

The uncertainties in results of a propagation model depend to a large degree on uncertainties in the environmental characteristics. The feasibility of developing models for bearing error and travel time error for infrasound sensors based on the techniques developed for the HydroCAM hydroacoustic model [Farrell and LePage, 1996] was evaluated. However, statistics of the atmospheric infrasound propagation environment are not as well known or as stable as those of the ocean environment.

Historical temperature and wind data were considered for use in determining statistics of the propagation environment. Certain of the assimilated data sets discussed above contain variance estimates of winds and temperatures; however, these estimates generally do not extend to sufficiently high altitudes for the variability of the infrasound propagation environment to be adequately assessed. Informal technical collaboration during this effort with Dr. Douglas Drob of the Naval Research Lab, who is currently investigating variance in atmospheric data, resulted in the definition of stochastic techniques to estimate realistic wind perturbation profiles.

A Monte Carlo approach to assessing the variability of both bearing and travel time was developed for infrasound propagation paths, based on application of ray tracing through a perturbed set of atmospheric profiles. This stochastic approach has the advantage of allowing flexibility in the choice of wind perturbation spectra, so the sensitivity of localization parameters to realistic characterizations of environmental variability can be assessed. The technique has been implemented so that it can be applied to any infrasound station in a user-defined network. Understanding variability in propagation paths is a necessary step in the development of a complete infrasound network model.

3.4 Software Implementation.

The development of the infrasound software tool kit followed an approach analogous to that used for the Hydroacoustic Coverage Assessment Model (HydroCAM) [Farrell and LePage, 1996], which was developed under the Department of Energy's CTBT R&D program. The HydroCAM software contains the best available seasonal databases of the ocean environment from the US Navy, the National Oceanic and Atmospheric Administration (NOAA) and other institutional sources, and is used to predict hydroacoustic travel time, amplitudes, travel time variances and network performance throughout the world's oceans.

Previous efforts at BBN, including HydroCAM, have produced a flexible software architecture for the manipulation and visualization of environmental data. For example, approximately 20 oceanographic and meteorological databases are currently accessible by the database software, and complex sound speed profile databases can be assimilated and interpolated to create sound speed fields for use as inputs to propagation models. This architecture was used during the infrasound development to rapidly provide an integrated database access and analysis capability. A goal for the infrasound software development was to maintain a flexible infrastructure so that additional models or databases could be added at a later time in order to improve functionality.

The infrasound software package was rapidly prototyped to develop a baseline functional capability. First, a detailed system block diagram was developed. The software design philosophy was to use existing models, databases and access software whenever possible. The

graphical user interface (GUI), including forms and data display formats, was designed and implemented using MATLAB[®].

Models and databases were identified and prioritized for integration by using a benefit/cost tradeoff. The benefits included the ability to meet operational requirements and acceptance by the infrasound research community. The cost included the estimated integration effort and computational requirements. As functions and models were added, each new capability was tested to determine accuracy and to assess functionality. More complex models were integrated and tested as justified by the fidelity of the results. Once the models were integrated with the environmental databases, they were exercised to determine sensitivity of propagation paths to the primary input parameters. As integration of the modeling components progressed, enhancements were added to the software to simplify and speed execution.

Measured infrasound data sets were obtained from a number of sources. Reports describing historical events of interest were provided by AFTAC and LANL. Data from recent events were obtained from the prototype International Data Center (IDC). Information in the open literature was also reviewed. Models were exercised, and results were compared to measurements for a subset of the available measured data.

Feedback on the software was obtained from experts in the community. A program review was scheduled in order to discuss development plans and agree on priorities. Beta testing of a prototype version of the software was conducted by experts at AFTAC and LANL. Following the testing, priorities for remaining development efforts were agreed in consultation with the experts.

Section 4

Results and Discussion

Results obtained during this effort are discussed in this section. Accomplishments include development of the integrated software and application of the tool to selected problems of interest. First, the capabilities of the software are discussed. Next, reports and presentations that were completed during the effort are summarized. Following this, examples of analyses that have been conducted using the software are presented, specifically, sensitivity studies, validation efforts, and example applications.

4.1 InfraMAP Software Tool Kit.

An integrated software package for infrasound modeling was developed during this effort.

A prototype (beta-release) of the model was provided to two locations (AFTAC and LANL) as part of the development process. BBN provided support to these users by (1) installing the software at the user location, (2) providing limited training on the use of the software, (3) adding capability as requested by the users and (4) fixing software errors as required. Feedback and recommendations provided by the users were incorporated in the software before the final release.

The software contains tools for modeling infrasound propagation through a dynamic atmosphere and for visualizing modeled propagation results and atmospheric characteristics. The atmospheric models, acoustic propagation codes, and display functions are integrated in a common software environment that allows for user-friendly data access and model execution.

The tool kit, called InfraMAP, for Infrasonic Modeling of Atmospheric Propagation, is a systems analysis tool that enables the user to perform propagation studies over global scales and at infrasonic frequencies. It can be applied to predict travel times, bearings, and amplitudes from potential event locations worldwide.

The InfraMAP user interface runs as a MATLAB application on UNIX-based workstations. It contains an assortment of databases, infrasound propagation models, and software for visualizing and interpreting results at each stage in the prediction process. The components of InfraMAP are in a variety of data formats and software languages: FORTRAN 77, FORTRAN 90, C++ and MATLAB script. The user interface makes all of this transparent and provides a capability to perform the following functions:

- Access, analyze and display a variety of environmental models.
- Evaluate global-scale infrasonic propagation using various modeling techniques.

The software design enables a user to run propagation models quickly and efficiently via pre-defined menus, and simultaneously provides flexibility both in the choice of model parameters and by allowing user-defined manipulation of data via the command line input.

Operation of InfraMAP is based on a graphical user interface (GUI) consisting of:

- A main window,
- Pull-down menus, and
- Forms (new menus that appear based on selections made in the main window).

Menus are organized by task for the most common operations, and are divided into the categories of “Environment” and “Propagation.”

- An Environment menu allows the user to visualize the atmospheric characterizations, either versus a spatial dimension or versus a temporal or geophysical model parameter.
- A set of three Propagation menus allows the user to define a scenario and execute InfraMAP’s integrated modeling capabilities.
 - a) A Propagation Scenario menu is used to select source and receiver locations, event date and time, and environmental parameters.
 - b) A Propagation Model menu is used to select the propagation model and its required input parameters. Default values of model parameters are provided automatically but can be modified by the user.
 - c) A Propagation Run/View menu is used to commence model execution and to display results on completion of a run. Model results are automatically stored and can be recalled later for analysis or display. A range of display options is available.
- A Propagation Variability menu is used to set up and run a Monte Carlo perturbation analysis of two ray parameters: azimuth deviation and travel time.

Additional functions such as printing, zooming, adding overlays, etc. are also available. Graphical representations of output data are displayed as MATLAB figures.

Operation of the software is fully described in a User’s Manual [Norris *et al.*, 1999], which was prepared as part of this effort. The manual includes instructions for installing and using the software.

4.2 Environmental Characterization.

The baseline environmental characterizations that are available for display and that have been integrated with the propagation models in InfraMAP are:

- the Horizontal Wind Model (HWM) [Hedin *et al.*, 1996] and
- the Extended Mass Spectrometer - Incoherent Scatter Radar (MSIS or MSISE) temperature and density model [Picone *et al.*, 1997].

HWM provides zonal and meridional wind components, and MSISE provides temperature, density and atmospheric composition.

4.2.1 Horizontal Wind Model (HWM).

HWM is a comprehensive empirical global model of zonal and meridional wind components that is based on accumulated measurements using a variety of techniques, including satellite, radar, and ground-based optical measurements. The model is used to determine winds while accounting for time, space, and geophysical variations. It provides a comprehensive statistical mean estimate based entirely on observational data.

Inputs into HWM include day of year, local time, latitude, longitude, altitude, solar flux, and geomagnetic activity. The first edition of the model, released in 1987, was intended for modeling of winds above 220 km and was built from wind data obtained from the AE-E and DE-2 satellites. The model was later extended down to 100 km by including wind data from ground-based incoherent scatter radar and Fabry-Perot optical interferometers, as well as MF/Meteor data. In 1993, HWM was extended down to the ground.

4.2.2 Mass Spectrometer - Incoherent Scatter Radar Atmospheric Model (MSIS).

The MSIS empirical model provides temperature, density and atmospheric composition based on in-situ data from seven satellites and numerous rocket probes. They provide predictions of temperature, and the densities of N₂, O, O₂, He, Ar, and H. Low order spherical harmonics are used to describe the major variations throughout the atmosphere including latitude, annual, semiannual, and simplified local time and longitude variations. These models facilitate data comparisons and theoretical calculations requiring a background atmosphere.

The MSIS model uses a Bates temperature profile as a function of geopotential height for the upper atmosphere and an inverse polynomial in geopotential height for the lower atmosphere. Exospheric temperature and other key quantities are expressed as functions of geographical and solar/magnetic parameters. These temperature profiles allow for exact integration of the hydrostatic equation for a constant mass to determine the density profile, based on a density specified at 120 km, as a function of geographic and solar/magnetic parameters.

4.2.3 Additional Environmental Data.

Topography

Topographic and bathymetric databases in InfraMAP are based on standard products from NOAA. The primary database is known as ETOPO (Earth TOPOgraphy) and is available at two resolutions: ETOPO30 (30 minute resolution); and ETOPO5 (5 minute resolution). An option for displaying topography in an azimuthally equidistant projection is offered.

Solar/Magnetic Indices

The variables F10.7, F10.7A, and A_P are used as input to the HWM and MSIS models.

- A_P is the planetary equivalent amplitude of daily geomagnetic disturbance,
- F10.7 is the daily solar radio flux at 10.7 cm, adjusted to 1 AU, and

- F10.7A is the 81 day average of F10.7 values, centered on the day of interest.

Further documentation describing these parameters, along with archives of historical values, are available online at the National Geophysical Data Center (NGDC). Default values are provided in InfraMAP.

Temperature/Wind Options

InfraMAP provides the software infrastructure to integrate additional atmospheric characterizations with the propagation models. Existing options in the software include: a linear temperature profile, a linear wind profile, a logarithmic wind profile, and user-defined data files of temperature and/or wind speed. InfraMAP contains a list of 1,676 locations where radiosonde data are collected. Further documentation describing radiosonde data, along with archives of historical values, are available online at the National Climatic Data Center (NCDC).

Examples

To view results of an environmental model, a user chooses the variable of interest, temporal and spatial parameters, resolution, and the type of data plot desired. Examples of output from the environmental models are presented in Figures 1 and 2. Figure 1 shows a global image of wind magnitude at a fixed altitude of 120 km, with wind vectors superimposed. Figure 2 displays temperature profiles at 500 km increments along a great circle path from the equator to the north pole.

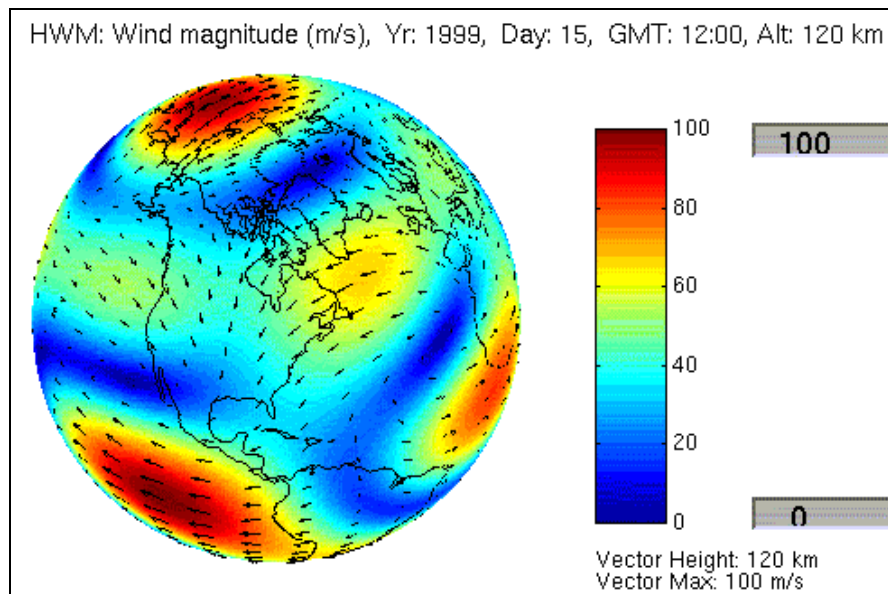


Figure 1. Global display of wind magnitude at fixed altitude (from HWM).

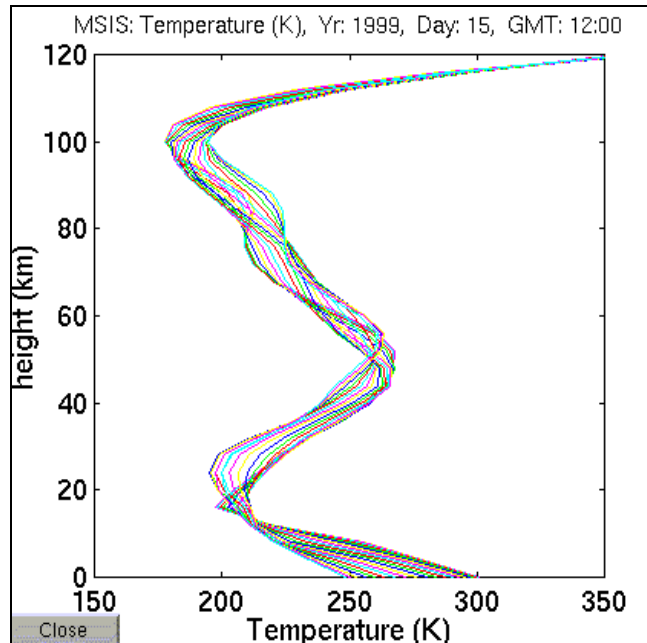


Figure 2. Temperature profiles at locations along a path (from MSISE).

4.3 Propagation Models.

The baseline set of acoustic propagation models contained in InfraMAP consists of:

- **Ray Tracing:** a three-dimensional ray theory model, HARPA (Hamiltonian Ray-Tracing Program for Acoustic Waves in the Atmosphere) [Jones *et al.*, 1986],
- **Normal Modes:** a WKB version [Dighe *et al.*, 1998; Hunter and Whitaker, 1997] of the normal mode model [Pierce and Kinney, 1976; Pierce *et al.*, 1973; Pierce and Posey, 1970], and
- **PE:** a continuous-wave, two-dimensional parabolic equation (PE) model [Jensen *et al.*, 1994; West *et al.*, 1992].

InfraMAP provides integration of these three models with the environmental characterizations described above. Source and receiver locations, date, and time-of-day can be selected to define the scenario of interest. The use of each model requires selection by the user of various model parameters; however, guidance is provided in the form of default values that were selected during the course of the software development.

Capabilities and characteristics of the propagation modeling techniques are summarized in Table 1. Sample output from the three models is shown in Figures 3 through 5.

Table 1. Capabilities and characteristics of propagation models.

Model	Travel Time	Azimuth Deviation	Absorption	Amplitude	Waveform	Horizontal Refraction/ Translation	Range Dependent	Reciprocal	Bandwidth
Ray Tracing (3-D)	Y	Y	Y	N	N	Y	Y	Y	N/A
Normal Modes (WKB)	Y	N	N	Y	Y	N	N	N	Broad
Parabolic Equation (2-D)	N	N	N	Y	N	N	Y	N	Single Freq.

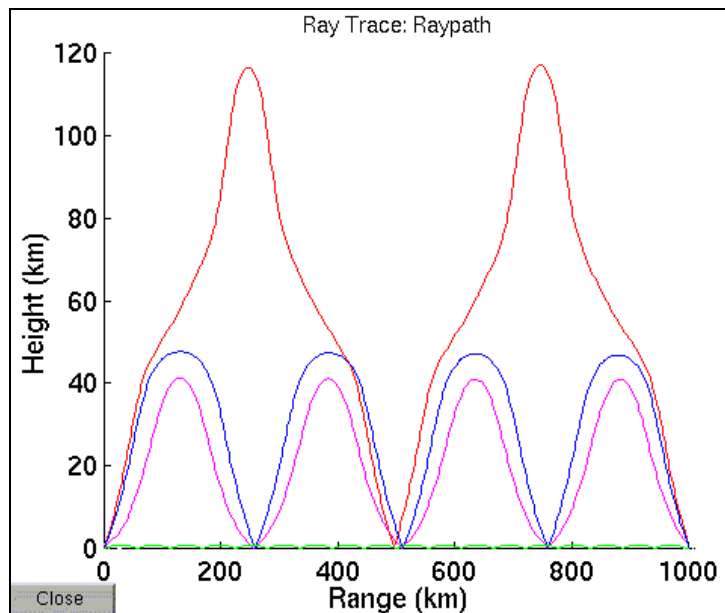


Figure 3. Vertical projection of ray paths (Eigenrays).

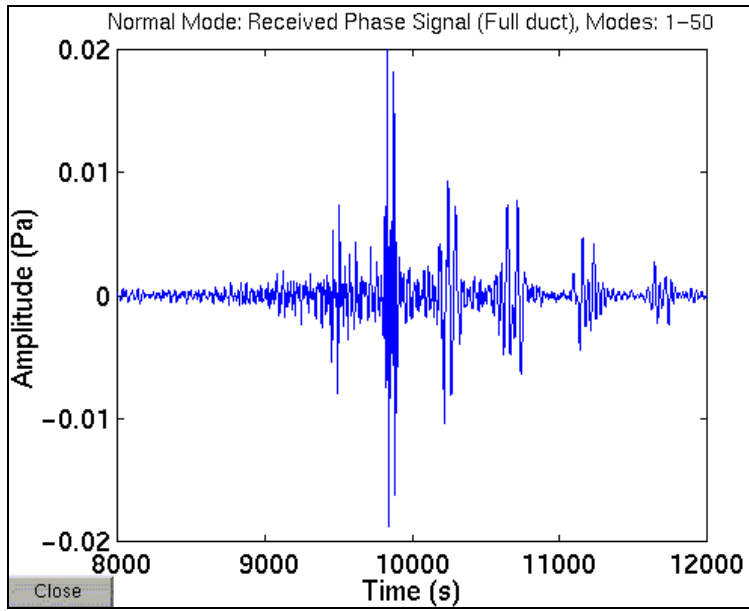


Figure 4. Waveform calculated using normal modes.

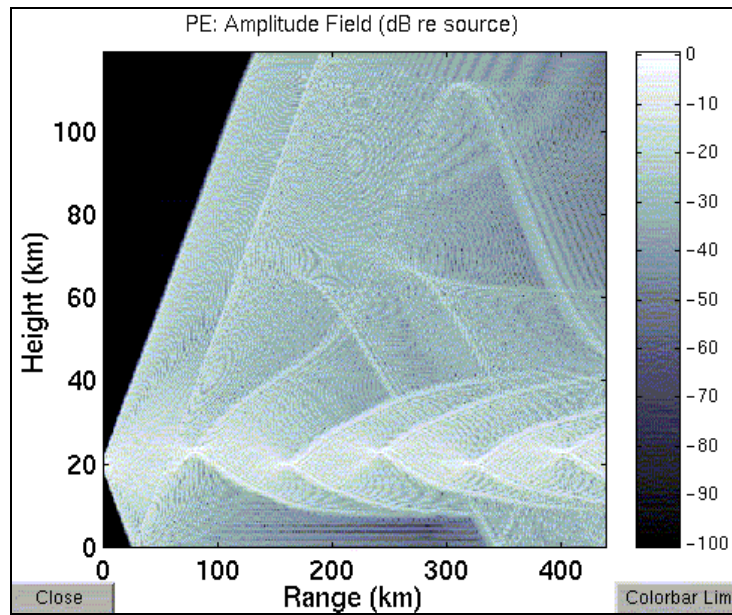


Figure 5. Amplitude field from parabolic equation model.

4.3.1 Ray Tracing.

The ray tracing code incorporates a range-dependent atmosphere in propagation calculations. It is defined in a three-dimensional domain using spherical coordinates. In addition to vertical and horizontal refraction, the model accounts for horizontal translation of the ray path due to the moving medium. A spherical earth model is used to determine range, and interaction with the surface is handled with specular reflections. Azimuth and elevation angles, travel time, and absorption can be calculated at each point along a ray path. The model predicts ray path attenuation due to viscous and thermal losses.

A single ray or a “fan” of rays can be launched from any given point. The ray tracing technique is capable of stepping either forward from a source or backward from a receiver. An option for "Reversing Propagation from a Receiver" is included in the software; when this option is selected, rays are "launched" from the receiver through an inverted propagation environment.

During this effort, an algorithm for finding eigenrays, rays that connect a source and a receiver to within a specified tolerance, was developed and implemented in InfraMAP. In the eigenray mode, an iterative algorithm is employed to search for rays that connect a source and receiver location to within a tolerance of a user-defined distance. The algorithm utilizes a shooting method to launch rays at various elevations and azimuths until eigenrays are identified.

A plotting option was also developed for the display of ray paths on an azimuthally equidistant projection.

4.3.2 Normal Modes.

A version of Pierce’s normal mode code, modified to determine propagation of higher frequency modes, is integrated into InfraMAP. The model uses the Wentzel-Kramer-Brillouin (WKB) method to calculate a dispersion curve, which in turn is used to calculate a received waveform, comprised of a finite sum of modal solutions, at a given range and azimuth.

Only range-independent environments are supported. The environmental profiles can be retrieved from the source location, receiver location, or from averaged values along the entire path.

An option is offered for solution of the set of dispersion curves only. In this case, full calculation of the received waveform is not performed.

InfraMAP can automate the selection of the waveform time window, calculated from a specified signal velocity and range. In addition, the special case of dual-duct propagation is identified and automatically processed, in which case the full waveform solution is the sum of the upper and lower duct solutions.

4.3.3 Parabolic Equation.

A continuous-wave, split-step implementation of the wide-angle finite-difference Parabolic Equation (PE) model was developed during this effort for use in InfraMAP. The PE technique steps forward from a source, which is characterized by a starter field, and calculates an attenuation field useful for predicting amplitudes along a vertical slice of the atmosphere.

The 2-D model can accommodate a range-dependent atmosphere. It does not account for horizontal refraction and therefore cannot provide predictions of azimuth deviation.

A number of input parameters must be chosen, including frequency, number of steps per wavelength, normalized ground impedance, and maximum altitude. Data can be displayed as an amplitude field over a vertical slice of the atmosphere, or as amplitude vs. range at a fixed altitude. Amplitude is expressed in decibels (dB) relative to the pressure at the source.

4.4 Network Performance.

InfraMAP incorporates a number of tools that support the assessment of network performance. Networks consisting of any number of stations can be defined and saved. Such networks can include stations in the IMS network, which is predefined and available in InfraMAP, existing prototype stations, and user-defined locations.

The ray tracing option for launching fans of rays from a receiver rather than from a source provides a convenient method for modeling travel time and azimuth deviation from a wide range of potential source locations to a single known receiver location. This capability can provide the basis for developing a grid of travel time and bearing corrections corresponding to a specific scenario of interest.

The capability of identifying eigenrays allows the key parameters that affect source localization (travel time and azimuth deviation) to be predicted for a particular combination of source and receiver locations. This can be useful for testing hypotheses of source location based on single station observations.

The Propagation Variability menu provides the capability of performing a Monte Carlo perturbation analysis about a reference eigenray. There is a choice of analysis variables: either azimuth deviation or travel time. This analysis approach allows assessment of (a) the sensitivity of ray tracing calculations to variability in wind profiles, and (b) the resulting effect on the key parameters that affect source localization. The modeled distributions of propagation variables can be used in assessing areas of uncertainty in source location.

In the Propagation Variability analysis, the environmental perturbation fields are defined using a 1-D vertical wave number spectrum of the horizontal wind, and individual realizations of spatial fields are generated through a random-phase technique [Peitgen, H. and D. Saupe, 1998]. Wind

profiles are perturbed repeatedly, and a Monte Carlo simulation is executed where multiple rays are traced through the sum of mean and perturbed profiles, and ray parameters are calculated for each perturbation. The perturbation model generates a unique wind perturbation profile for each realization calculated.

- If azimuth deviation is chosen, then the wind component normal to the great circle path (crosswind) is perturbed and the wind component along the great circle path (headwind or tailwind) is not perturbed.
- If travel time is chosen, then the wind component along the great circle path (headwind or tailwind) is perturbed and the wind component normal to the great circle path (crosswind) is not perturbed.

The wind perturbation is based on a power spectral density (PSD). Default values of the power law exponent, the perturbation wavelength range (in km), and the PSD magnitude are provided. The user must specify the number of realizations in the Monte Carlo simulation.

Three output displays of analysis results are presented:

- Probability density function estimate,
- Density of calculated ray ground hit points as a function of range, and
- Locations of ray ground hit points (overlaid on an azimuthally equidistant projection of topography). Perturbed ray endpoints are shown compared to the ground hit point of the unperturbed reference ray.

Examples are shown in Figures 6 through 9. Figure 6 depicts a wind perturbation spectrum, and Figure 7 shows a realization of a perturbation profile calculated using this spectrum. Figure 8 is a plot of ray ground hit points resulting from a Monte Carlo simulation, and Figure 9 is the corresponding probability density function estimate.

The software provides the infrastructure to add additional capabilities to support network performance evaluation, for example, station detection characteristics, estimates of noise levels, area of uncertainty estimates, etc.

4.5 Reports to the Research Community.

As required under the contract, BBN personnel attended both the 20th and 21st Annual Seismic Research Symposia on Monitoring a CTBT. Papers were published in both proceedings [Gibson and Farrell, 1998; Gibson *et al.*, 1999], posters were presented at both meetings, and an InfraMAP software demonstration was presented at the 21st Symposium. A BBN technical memorandum was issued in December 1998 [Gibson *et al.*, 1998], documenting a portion of the poster that had been displayed at the 20th Symposium. In addition, a program review was held in December 1998 where interested parties provided feedback on the design of the developing software.

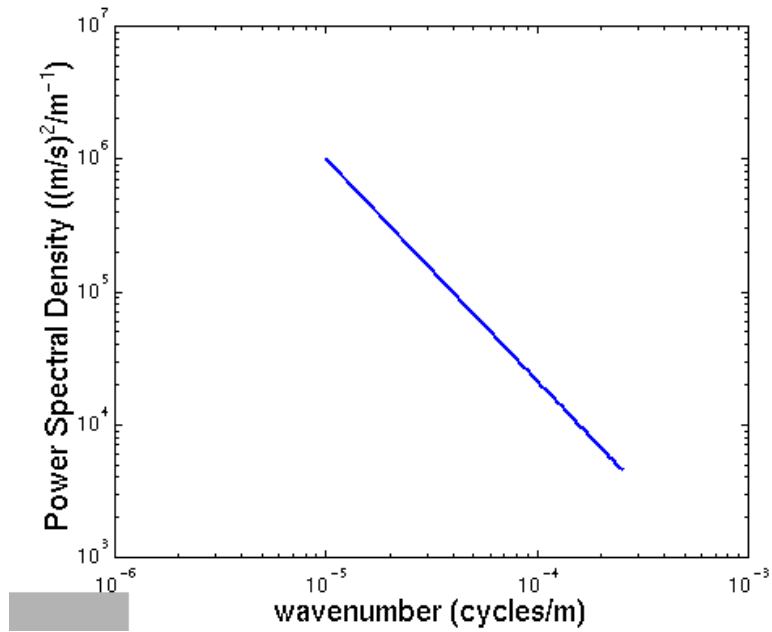


Figure 6. Perturbation spectrum.

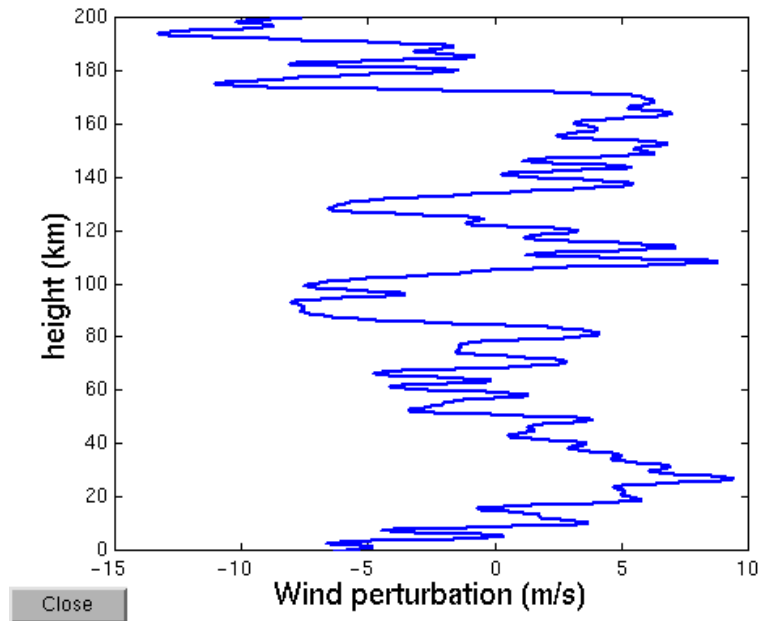


Figure 7. Perturbation profile.

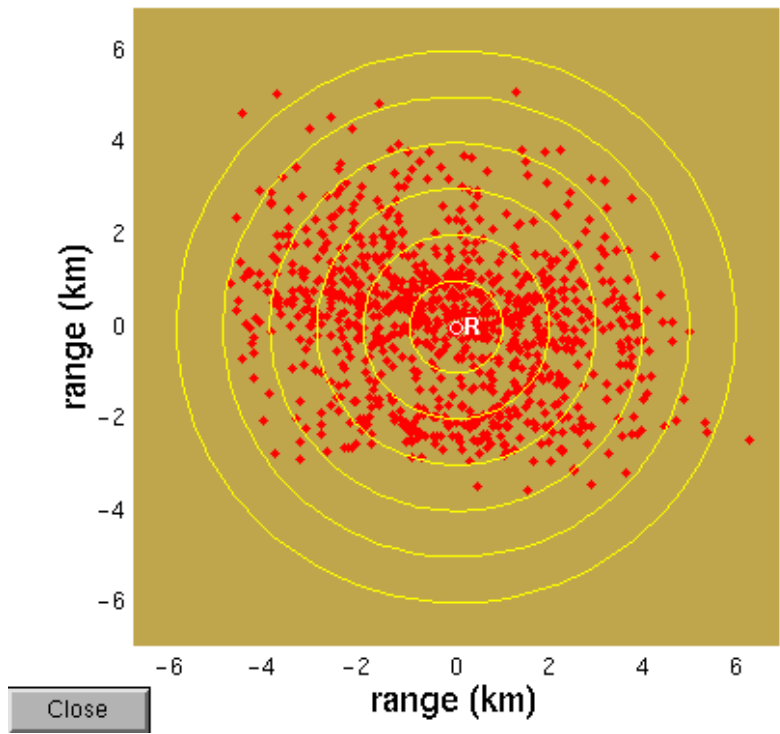


Figure 8. Ray ground hit points.

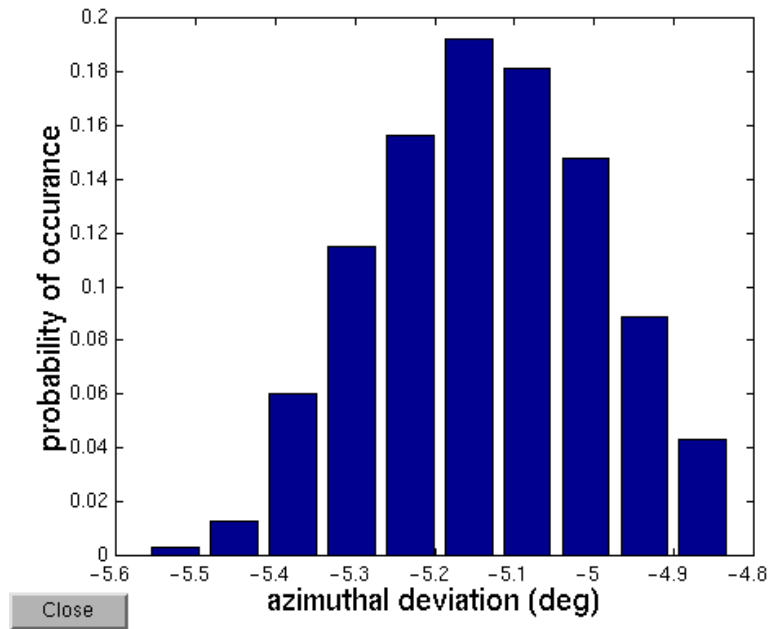


Figure 9. Probability density estimate.

The research program was summarized in a presentation to the CTBT Infrasound monitoring community at the Informal Workshop on Infrasound, held in France in July 1998 [Gibson, 1998]. Specific research results were presented at the 1999 Spring Meeting of the American Geophysical Union (AGU), during a special session on Infrasound [Norris and Gibson, 1999a], and at the 138th meeting of the Acoustical Society of America in Fall 1999 [Norris and Gibson, 1999b].

4.6 Sensitivity Analyses.

The InfraMAP tool kit allows sensitivity analyses to be conducted readily. Model parameters can be varied systematically in order to compare results from a range of propagation scenarios. Such studies are useful for assessing the accuracy, flexibility, and robustness of different modeling approaches and for defining spatial and temporal resolutions required for accurate predictions of infrasound travel times, bearings, and amplitudes. They can also be used to identify systematic biases in travel time and azimuth that it may be possible to eliminate in a localization technique.

As discussed above, the selection of certain input parameters, e.g., step size, is required for successful operation of the propagation models. Models were tested and sensitivity studies were performed during the software development phase in order to determine appropriate default values for these parameters for use in InfraMAP's user interface. These tests are not described in detail in this report.

Examples of analyses that have been conducted during the effort addressing the sensitivity of propagation results to environmental parameters are presented here.

4.6.1 Diurnal Sensitivity.

A sensitivity study was carried out to evaluate the effect of diurnal variability of atmospheric winds and temperature on ray paths. Four source-receiver geometries were studied.

- Two geometries had a source location in Central Asia (50.5 N, 78.0 E). One receiver was 2500 km west at a bearing of -90 degrees, and the other was 2500 km North at a bearing of zero.
- Two geometries had a source location in Nevada (38.7 N, 115.8 W). One receiver was 1000 km east of the source at a bearing of 78 degrees, and the other 1000 km north at a bearing of zero.

For these event scenarios, the time of year was mid-September. Specific attention was given to azimuthal deviation and travel time, as these ray parameters impact localization algorithms.

Example results from the 2500 West path from the Central Asia source are given in Figures 10 and 11. Five eigenrays were identified and all had turning points in the thermosphere at altitudes in the range 110-130 km. Over the 24-hour period of the sensitivity study, the travel time variability was up to 2.3% and the change in azimuthal deviation was up to 4.3 degrees. The diurnal variability in temperature was small and found to have a negligible impact on the

eigenrays. However, changes in the zonal and meridional winds were significant; winds at the source location are shown in Figures 12 and 13. The greatest variability occurs above 100 km, where the effects of the semi-diurnal solar tide are apparent.

The travel along a ray path is directly influenced by the projected wind along the path; the wind subtracts or adds to the effective sound speed depending on wind direction. This property is observed in the high correlation between the zonal wind and travel time. For example, the ray travel times reach a maximum for events at 10-11 UT. This correlates with the minimum extreme in the eastward zonal wind above 100 km. Westward ray paths at this time of day encounter a headwind with a maximum speed of 60 m/s at their turning points. Similar observations can be made regarding the azimuthal deviations. The crosswind along a ray path acts to translate and/or refract the path, resulting in a change in the observed azimuthal deviation at the receiver. Maximum azimuthal deviation in the negative direction occurs for events at 6 UT. This correlates with the maximum in the meridional winds above 100 km. Ray paths at this time of day encounter a maximum crosswind of 60 m/s at their turning points.

Similar conclusions were drawn from the study of the Nevada source geometries. The diurnal variability of ray travel time, signal velocity, and travel time are summarized in Table 2 for all four geometries.

Table 2. Summary of diurnal variability results for four geometries.

Western US Path	Eigenrays	Diurnal change in:		
		Travel Time ($\pm\%$)	Signal Velocity (m/s)	Azimuthal Deviation (deg)
North	Stratospheric	–	–	–
	Thermospheric	1.2 – 1.9	7 – 9	1.0 – 3.0
East	Stratospheric	0.2 – 0.4	1 – 3	0.1 – 0.8
	Thermospheric	1.6	9	2.8

Central Asia Path	Eigenrays	Diurnal change in:		
		Travel Time ($\pm\%$)	Signal Velocity (m/s)	Azimuthal Deviation (deg)
North	Stratospheric	–	–	–
	Thermospheric	1.7 – 1.9	~3	0.5 – 1.7
West	Stratospheric	–	–	–
	Thermospheric	1.3 – 2.3	2 – 4	1.5 – 4.3

In summary, it is concluded from the diurnal sensitivity study that modeled diurnal changes in winds can generate observable changes in travel time and azimuthal deviations for ray path solutions over fixed source-receiver geometries. These changes correlate strongly with the wind at the ray turning points. Only thermospheric rays are discussed here. Similar, although weaker, diurnal effects were also found to hold for stratospheric rays [Norris and Gibson, 1999a].

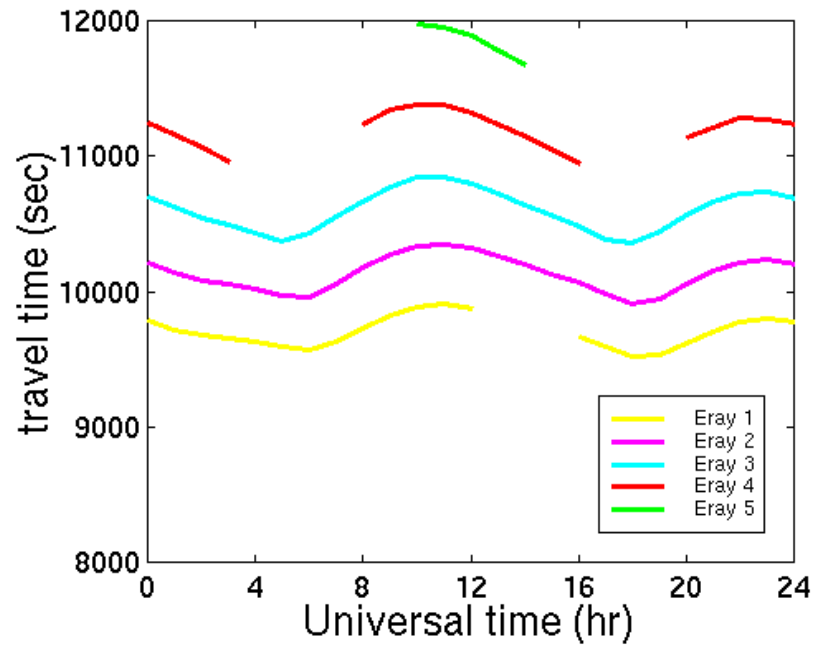


Figure 10. Travel time variations over diurnal cycle; 2500 km path.

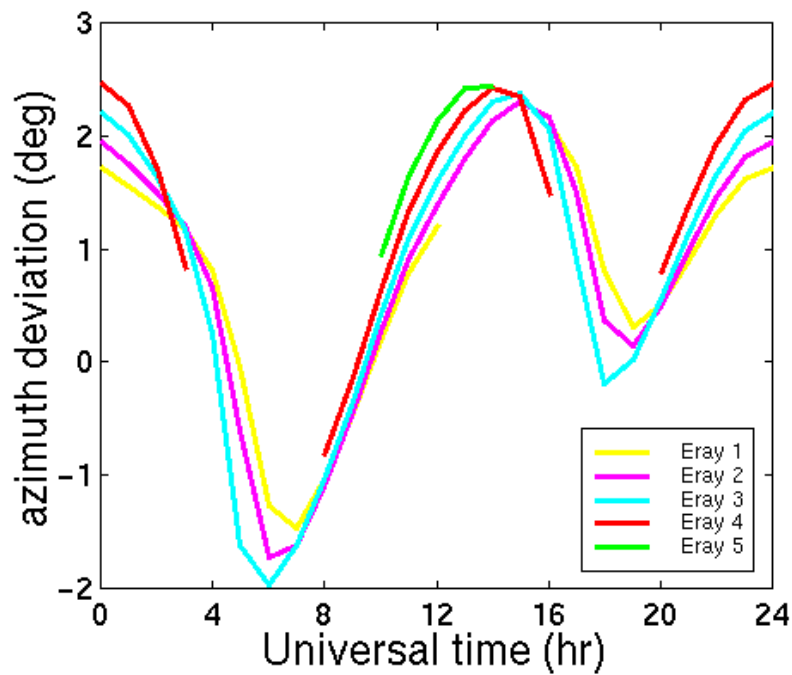


Figure 11. Azimuth deviation variations over diurnal cycle; 2500 km path.

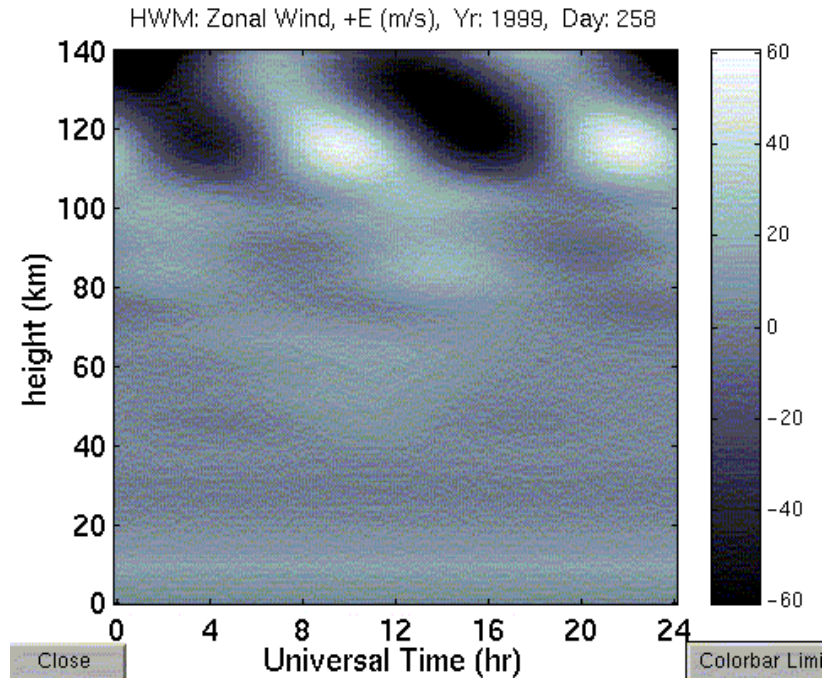


Figure 12. Zonal wind variations over diurnal cycle; Central Asia (+Eastward).

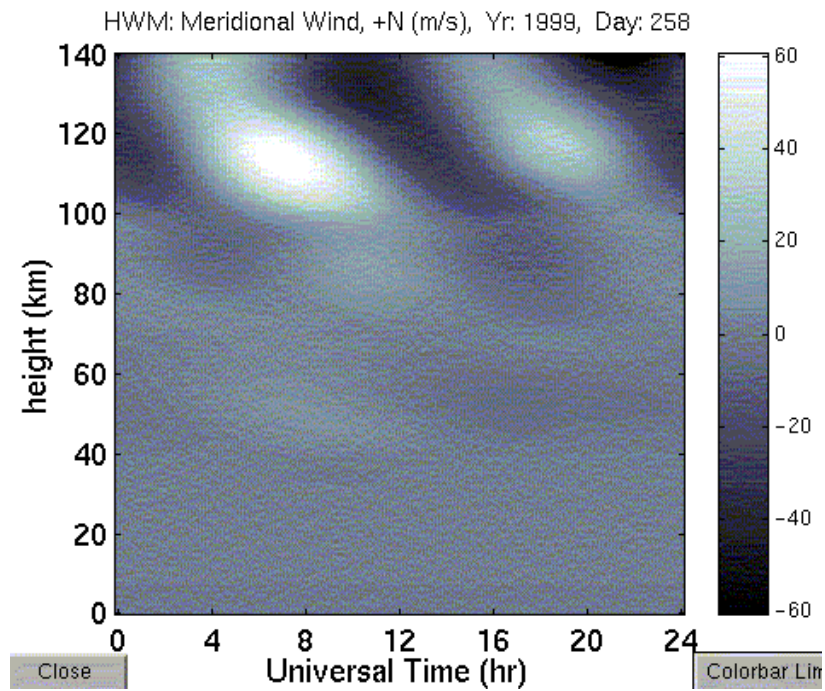


Figure 13. Meridional wind variations over diurnal cycle; Central Asia (+Northward).

4.6.2 Seasonal Sensitivity.

A sensitivity study was also carried out to evaluate the effect of seasonal variability of atmospheric winds and temperature on ray paths. The identical Western US source-receiver configuration to that in the diurnal sensitivity study was used here. The time of day was held constant at 12 UT, and the time of year was varied over a full year in 15-day increments.

The winds again dominate the propagation characteristics. Figures 14 and 15 give the zonal and meridional wind profiles at the source as a function of calendar day. The dominant feature is the strong zonal wind at stratospheric heights of 40-60 km. In the winter, these winds are eastward with a magnitude of approximately 60 m/s. In the summer, the stratospheric wind reverses to a 60 m/s westward flow.

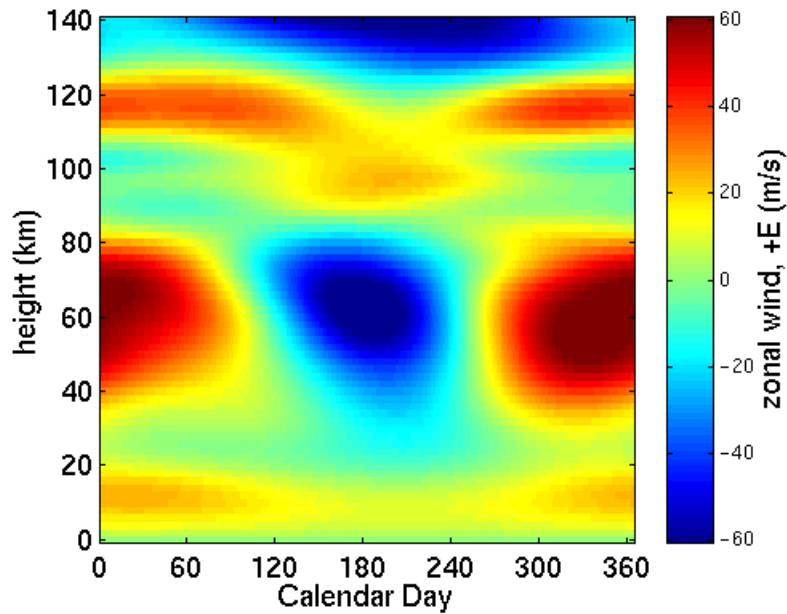


Figure 14. Zonal wind variations over diurnal cycle; Nevada (+Eastward).

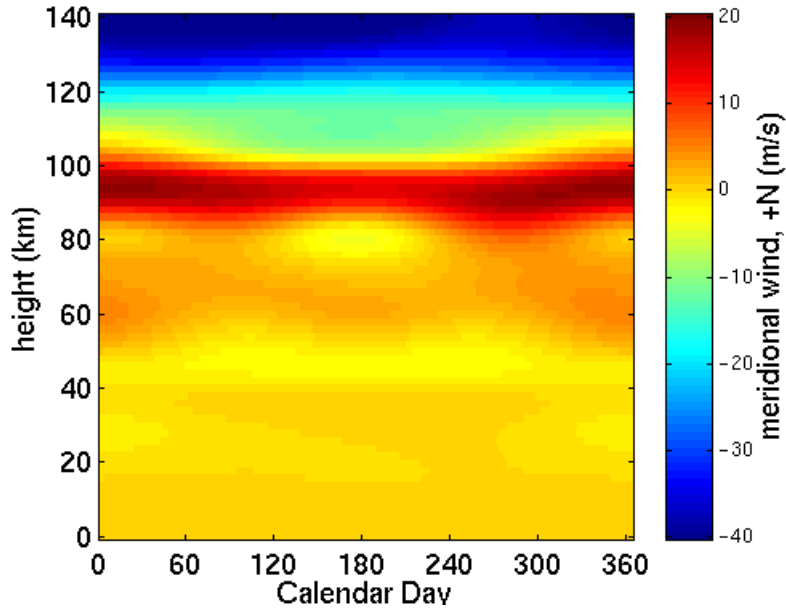


Figure 15. Meridional wind variations over diurnal cycle; Nevada (+Northward).

For the East path, both stratospheric and thermospheric eigenrays were identified. The stratospheric paths only exist in the winter period when the stratospheric winds create a lower propagation duct. The eigenrays found at calendar day 301 are shown in Figure 16. The reversal of wind direction results in a large deviation in travel time for the thermospheric rays. The travel time difference between winter, when the stratospheric winds are in the direction of propagation, and summer, when they are against it, is approximately 600 sec. The seasonal travel time variability for all eigenrays is shown in Figure 17.

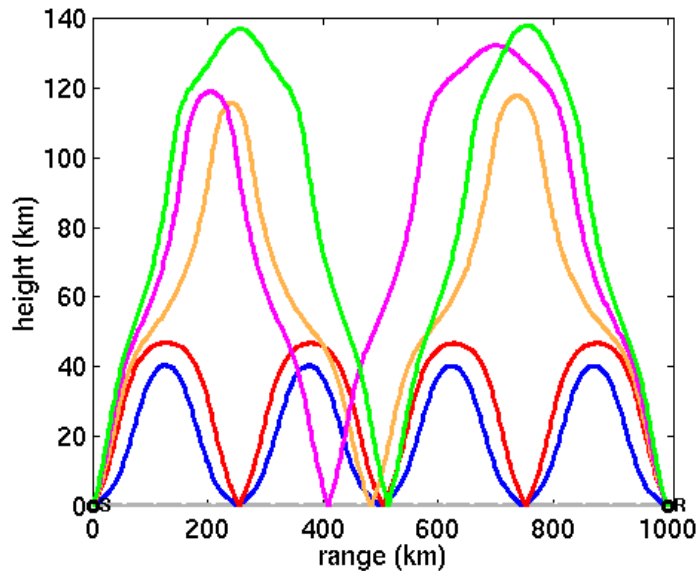


Figure 16. Eastward eigenrays from Nevada; Day 301.

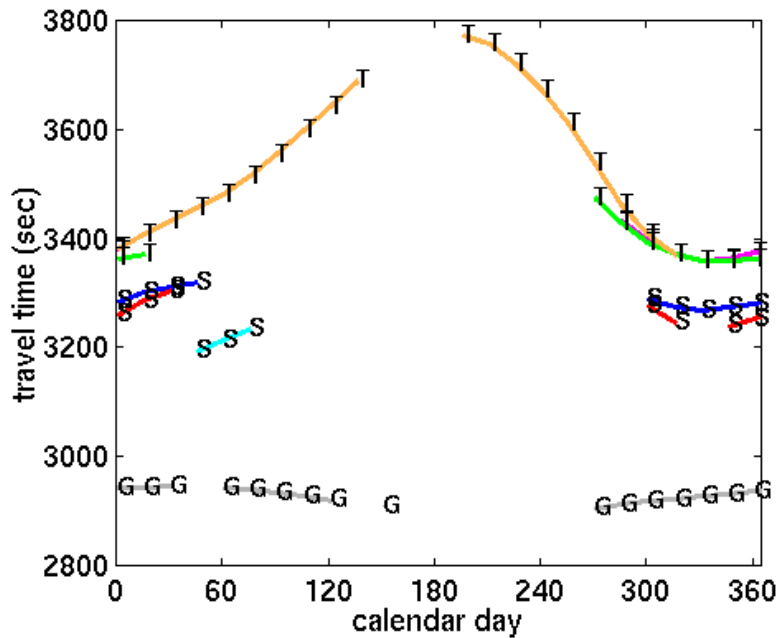


Figure 17. Travel time variations over annual cycle; 1000 km path.

For the North path, only thermospheric eigenrays are identified. The strong zonal winds result in large azimuthal deviations. Due to the zonal wind reversal in the stratosphere, the azimuthal deviation changes from a minimum of -6 deg in the winter to 3 deg in the summer. A summary of the seasonal variability for both North and East paths is given in Table 3.

Table 3. Summary of seasonal variability results for two geometries.

Western US Path	Eigenrays	Seasonal change in:		
		Travel Time ($\pm\%$)	Signal Velocity (m/s)	Azimuthal Deviation (deg)
East	Stratospheric	0.6 – 1.0	4 – 6	0.2 – 0.5
	Thermospheric	1.1 – 5.6	6 – 31	0.5 – 1.4
North	Stratospheric	–	–	–
	Thermospheric	0.2 – 0.4	1 – 2	5.0 – 8.7

This sensitivity study indicates that seasonal effects on 1000 km are significant. Travel time changes are on the order of 6%, and azimuthal deviation changes are on the order of 9 degrees. The magnitude of these changes indicates that seasonal effects must be accounted for in infrasonic localization algorithms to meet performance goals. As an example, for the East path, the $\pm 6\%$ change in travel time (assuming a signal velocity of 275 m/s) results in a receiver

localization uncertainty of 50 km. For the North path, the ± 4.5 deg change in results in a receiver localization uncertainty of 150 km. [Norris and Gibson, 1999b]

4.6.3 Sensitivity to Solar Magnetic Disturbance.

InfraMAP was used to evaluate the effect of variability in solar magnetic activity on ray paths. Geomagnetic disturbances from solar activity influence atmospheric temperature and winds at high altitudes. The planetary equivalent daily disturbance amplitude, A_P , is used as an input parameter in the wind and temperature models and it affects the modeled environment at altitudes above 100 km.

Archived values of A_P over a six-year period were reviewed to determine a realistic parameter range for the study.

- Values of A_P ranged from approximately 1 to 100.
- Approximately 97% of the days had A_P values of less than 50.
- 10% of the days had A_P equal to 4.

The values of A_P chosen for the study were: 4, 8, 16, 32, 64, and 128.

In the modeled scenarios, the source was located in Central Asia (50.5° N, 78.0° E), and the receivers were due West and due North at a range of 2500 km. The time of year was mid-September and the time of day was 12 UT. Five eigenrays were identified and all had turning points in the thermosphere at altitudes in the range 110-125 km. At these altitudes, modeled temperatures and winds are sensitive to solar effects.

The effects on travel time and azimuth deviation of the eigenrays are shown in Figures 18 and 19, respectively, for the northward path. Over the A_P range of the sensitivity study, the travel time variability was up to 2% for each ray path. This effect due to A_P is small compared to the range of travel times among the five rays. The change in azimuth deviation was up to 2 degrees, which is of the same order as the range among the five rays.

For this particular modeled event scenario, it is concluded that solar magnetic disturbance effects may result in observable changes to thermospheric ray paths but are unlikely to represent a large source of variability in propagation. However, the effect of A_P variability may be more prominent in other geographic regions or in other event scenarios.

4.6.4 Sensitivity to Latitude.

Atmospheric characteristics, particularly zonal winds, vary greatly depending on latitude. Monitoring stations in the IMS will be located at a wide range of latitudes. The effect of receiver latitude on key propagation parameters was studied for the case of northward propagation.

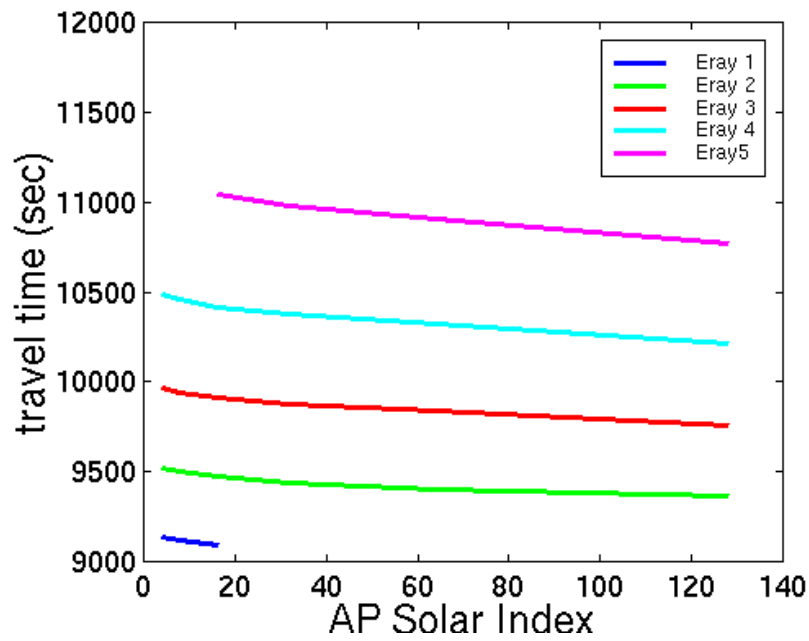


Figure 18. Travel time variability due to solar magnetic disturbance.

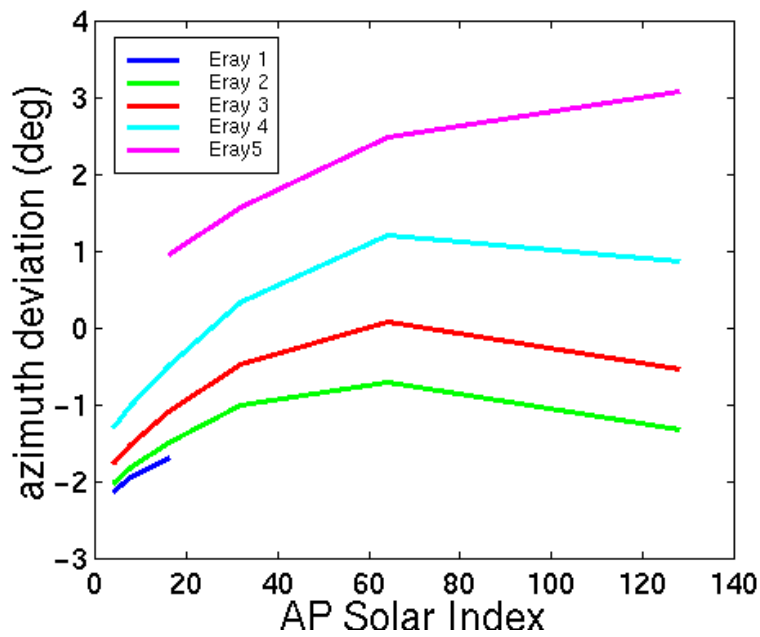


Figure 19. Azimuth deviation variability due to solar magnetic disturbance.

For the scenarios modeled in this study, the range from source to receiver was held constant at 2500 km. In all scenarios, the source and receiver locations were along the same meridian at longitude 78.0° E, with the receiver to the north of the source. The source and receiver latitude range for the study was from near the South Pole to near the North Pole. Latitude increments of 10 degrees were used in the study. The time of year was mid-September and the time of day was 12 UT.

The zonal winds in a slice of the atmosphere at longitude 78.0° E and from 0 to 120 km in altitude are shown in Figure 20. The slice extends from the South Pole (shown at 0 km) to the North Pole (shown at 20000 km). Positive values indicate eastward winds.

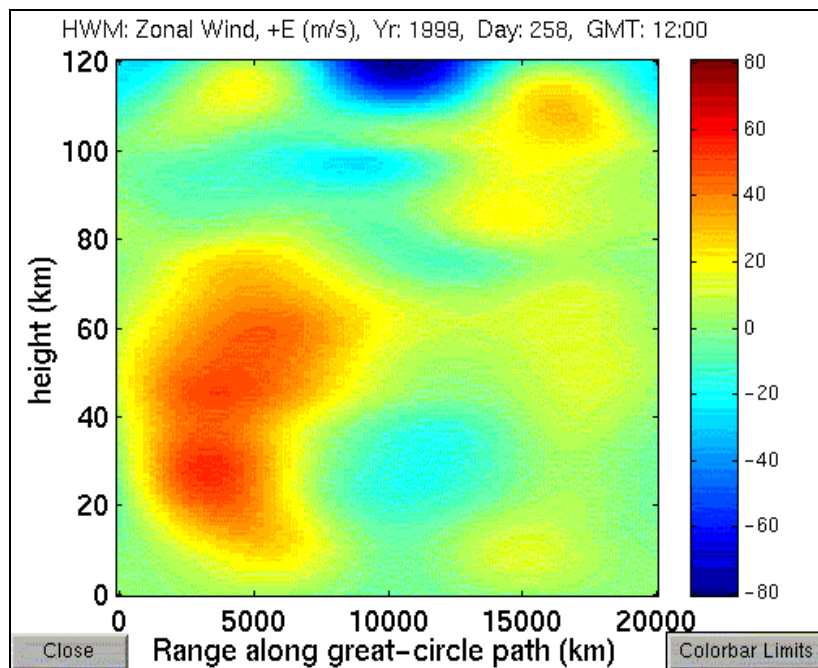


Figure 20. Zonal winds (+E) along slice of atmosphere from South Pole to North Pole, 78° E.

At stratospheric altitudes:

- Strong eastward winds are present in the Southern Hemisphere;
- Winds are westward near the equator (shown at approximately 10000 km range); and
- Relatively weak eastward winds are present in the Northern Hemisphere.

The zonal wind represents a crosswind for the northward propagation paths modeled in this study. It should be noted that there is an effective shift in the direction of the crosswind for propagation paths that cross over one of the poles; this is due to modeled wind circulation around the poles.

From two to five eigenrays with turning points in the thermosphere were identified for each path. Paths with turning points in the stratosphere were only identified near the South Pole. Travel time and azimuth deviation for each ray are shown as a function of source latitude in Figures 21 and 22, respectively. (Note: Paths with the source at 80° N traverse over the North Pole. Paths with the source indicated at -100° N traverse over the South Pole. The actual source location for this latter path is at approximately 80° S, 102° W, and the receiver location is at longitude 78° E.)

The modeled variability in travel time is small for this set of meridional paths. This is because the strong zonal wind represents a crosswind for these paths rather than a headwind or tailwind. Meridional winds are smaller in magnitude than the zonal winds and vary less with latitude. The cross-range translation of the rays due to the zonal wind does not have a large effect on travel time for these paths.

Conversely, the modeled variability in azimuth deviation is large for these paths. The change in modeled azimuth deviation over the range of this sensitivity study is approximately 8 degrees. The strong zonal wind represents a crosswind for these paths, and the high crosswinds result in large values of azimuth deviation. At those latitudes where zonal wind velocities are high in the eastward direction, azimuth deviation is negative, and vice versa.

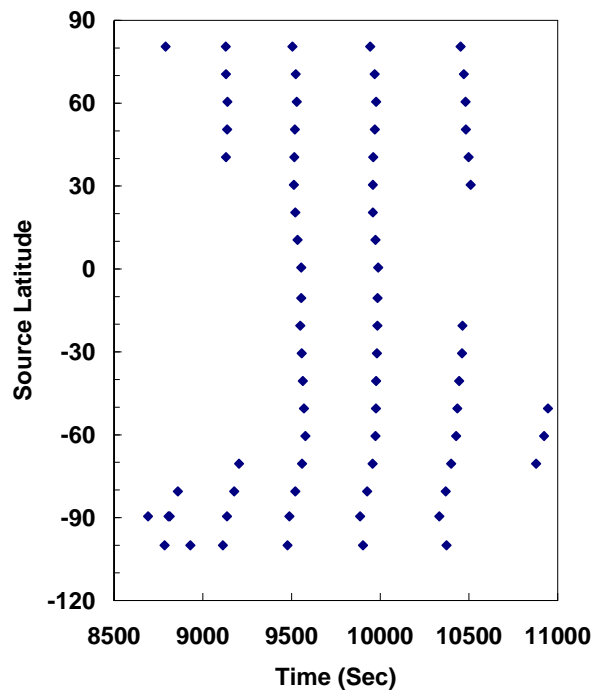


Figure 21. Variability in travel time due to source latitude; meridional path.

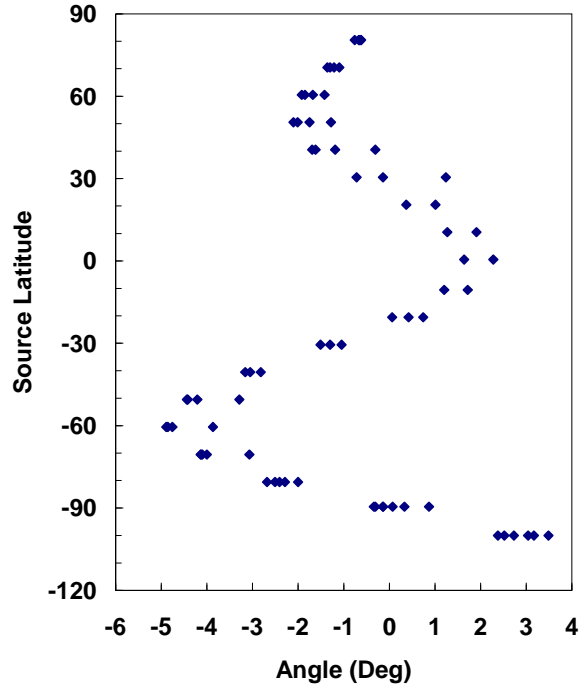


Figure 22. Variability in azimuth deviation due to source latitude; meridional path.

In summary, this study indicates that, for meridional propagation paths with thermospheric turning points, (a) zonal winds, which vary strongly with latitude, have a strong effect on azimuth deviation, and (b) changes in travel time resulting from high zonal winds are likely to be relatively small.

4.7 Validation Studies.

During the effort, data describing a number of historical infrasound events were obtained from various sources. These data were reviewed with scientists at AFTAC and LANL to determine an appropriate baseline measurement set for comparison with the model predictions. Additional measured data were obtained from the prototype IDC and from published literature.

For the data obtained from AFTAC and LANL, events were categorized by parameters such as source location, receiver location, range, time of year, and time of day. Data sets that had a reasonable distribution of events over a significant range of parameter values were identified for further study. Travel velocity, azimuth deviation and amplitude data were compiled for events by category. Diurnal and seasonal trends in travel velocity and azimuth deviation were examined. Events at several source and receiver locations were found to show seasonal trends. Events at one set of source and receiver locations were identified as showing diurnal trends in azimuth deviation. Ray tracing propagation modeling at a range of dates and/or times was conducted for several of the scenarios of interest. Comparisons between measurements and model predictions were generally favorable. Preliminary results from these investigations were presented at program reviews during this effort. These results are not presented in this report.

Comparisons between observations and predictions are presented here for one event: the meteor-fireball, or super-bolide, of 9 October 1997 above Horizon City, Texas, near El Paso, as observed at two locations. The primary objective of this case study was to assess the utility of three-dimensional ray tracing for predicting travel time and azimuth. The HWM and MSISE models were used to characterize the environment.

Infrasound from the bolide was observed at the two arrays at Los Alamos, NM and at the TXIAR array in West Texas. The atmospheric explosion was determined to have occurred at 18:47:15 UT at the location 31.8° N, 106.1° W and an altitude of 28-30 km, based on visual observations, satellite data and seismic signals [ReVelle *et al.*, 1998]. Four separate arrivals were associated with this event at both LANL [Armstrong, 1998] and TXIAR [Herrin *et al.*, 1998].

InfraMAP was used to identify eigenrays from the source location, at a height of 29 km, to:

- TXIAR, at a range of 359 km and a back azimuth of approximately 320°, and
- LANL, at a range of 453 km and a back azimuth of 177°, corresponding to near-northward propagation.

A tolerance or miss-distance of 5 km was allowed for each ray at the receiver. The rays represent distinct infrasonic “phases,” or separate bundles of energy that could constitute separate observed arrivals.

Vertical projections of five ray paths to TXIAR are shown in Figure 23. Two stratospheric rays and three thermospheric rays, two of which include a ground reflection, were identified. Vertical projections of three ray paths to LANL are shown in Figure 24. One stratospheric ray and two thermospheric rays, one with a ground reflection, were identified.

Table 4 compares the modeled travel time and azimuth deviation with those of the observed arrivals at TXIAR. The main arrival at 1239 seconds is well modeled as a stratospheric path. The arrival at approximately 1465 seconds is also well modeled as a thermospheric path with a ground bounce. The weak first phase was observed to arrive approximately 6% earlier than predicted. The predicted thermospheric phase at 1365 seconds was not reported as observed. The modeled azimuth deviations are within 1 degree of the observed deviations.

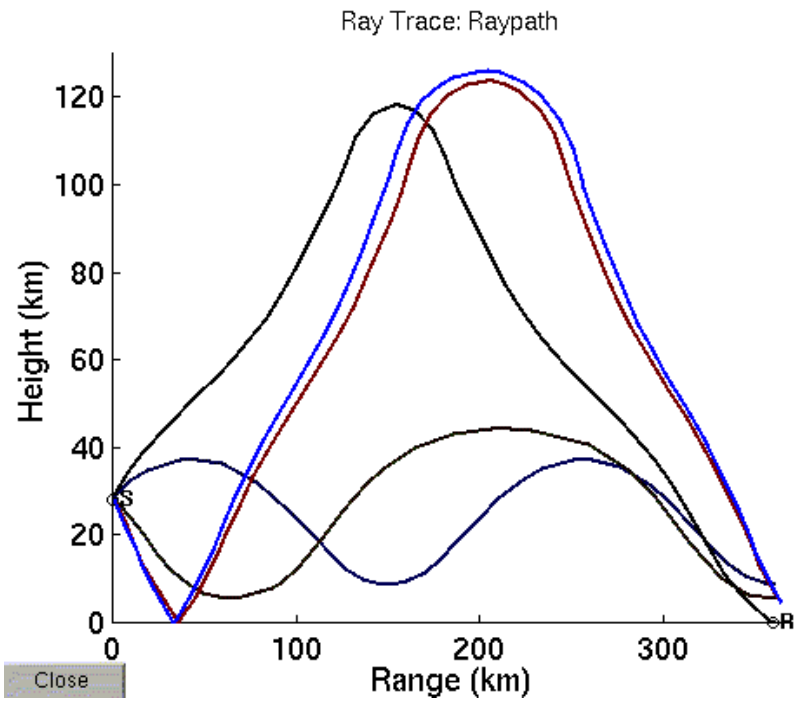


Figure 23. Modeled eigenrays from El Paso bolide to TXIAR array.

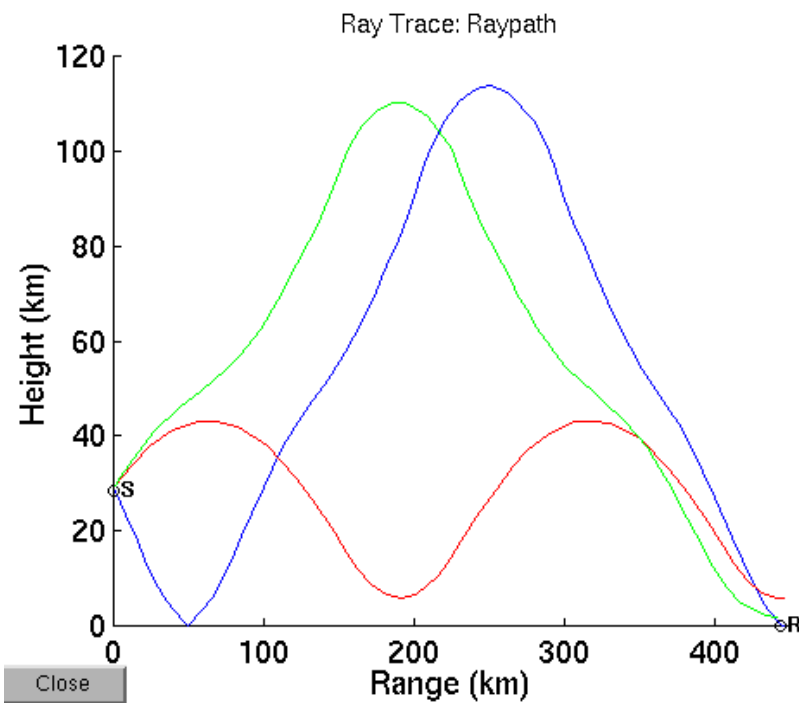


Figure 24. Modeled eigenrays from El Paso bolide to LANL array.

Table 4. Comparison of observed and modeled arrivals at TXIAR array.

Travel Time (seconds)		Azimuth Deviation (degrees)	
Observed	Modeled	Observed	Modeled
1139		+1.8	
	1211		+1.7
1239	1233	+1.2	+1.1
	1365		+3.4
1464	1475	+4.0	+3.2
1466	1476	+4.0	+3.2

Table 5 presents similar results for LANL. The main arrival at 1525 seconds is well modeled as a stratospheric path. The arrival at 1694 seconds is also well modeled as a thermospheric path with a ground bounce. The observed azimuth deviations are not well modeled; this may be due to variability in zonal wind.

Table 5. Comparison of observed and modeled arrivals at LANL array.

Travel Time (seconds)		Azimuth Deviation (degrees)	
Observed	Modeled	Observed	Modeled
1425		+3	
1525	1524	+3	-2.4
	1604		-3.1
1694	1695	+3	-2.9
1885		+3	

Efforts were also made to model propagation from the bolide event to LANL using *in situ* radiosonde data to define the environment. [Gibson *et al.*, 1998] The objective was to compare predicted propagation results using an empirically modeled characterization of the atmosphere with those using measured atmospheric data.

Measured data from a sonde at El Paso (at 11:00 UT) were used to define the environment up to 35 km, and values calculated from MSISE and HWM were used above 40 km. Values and derivatives of the model data were calculated at an altitude of 40 km, and a cubic spline was used to fit the modeled data above this point to the measured data below. Ray tracing was performed without range dependence.

Results using the modeled atmosphere and the “hybrid” atmosphere were compared for a stratospheric ray path. Differences in travel time were negligible. Azimuth deviation changed by less than 1 degree. In this particular case study, use of available *in situ* data did not have a major effect on propagation predictions; however, other scenarios may show larger effects.

4.8 Example Application.

In this section, the application of InfraMAP to a hypothetical source location problem is described.

4.8.1 Scenario.

Propagation paths were modeled from a location in the South Pacific (55.0° S, 132.0° W, 1 km altitude) to the nine nearest station locations in the IMS infrasound network. The location of the source was chosen such that the range to the nearest IMS station was approximately 3000 km. The most distant of the nine stations chosen was approximately 5000 km. Great circle paths from the source to the stations are shown in an azimuthally equidistant projection, with contours shown at 1000 km increments, in Figure 25. The stations in this study were:

Easter Island,	Windless Bight, Antarctica,
Juan Fernandez Island,	Chatham Island,
Paso Flores,	Tahiti,
Ushuaia,	Marquesas Islands.
Siple Station, Antarctica,	

The azimuths from source to receiver (with respect to true North) vary widely among the nine station locations.

Eigenrays through the modeled atmosphere were calculated for two days of the year: 1st January (Day 1) and 1st July (Day 182). Zonal winds above the source location are depicted over an annual cycle in Figure 26. Winds are strongly westward in winter (Day 1) and strongly eastward in summer (Day 182).

Several eigenrays were identified for each path. Travel time and azimuth deviation were calculated for each ray. Source-to-receiver range was divided by travel time to determine signal velocity for each ray.

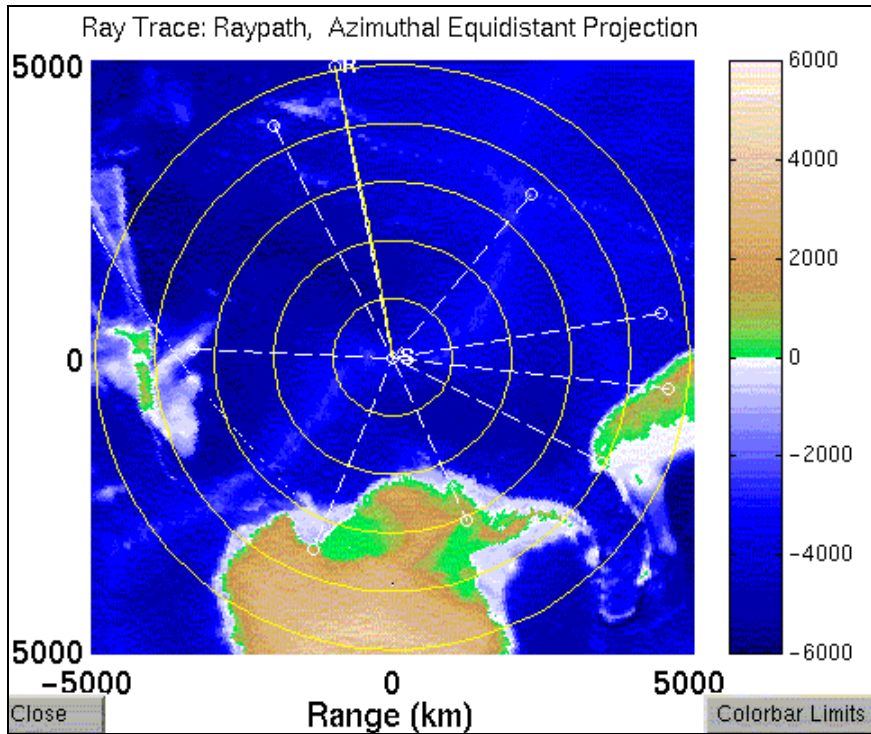


Figure 25. Paths from South Pacific source location to nine infrasound stations; 1000 km contours.

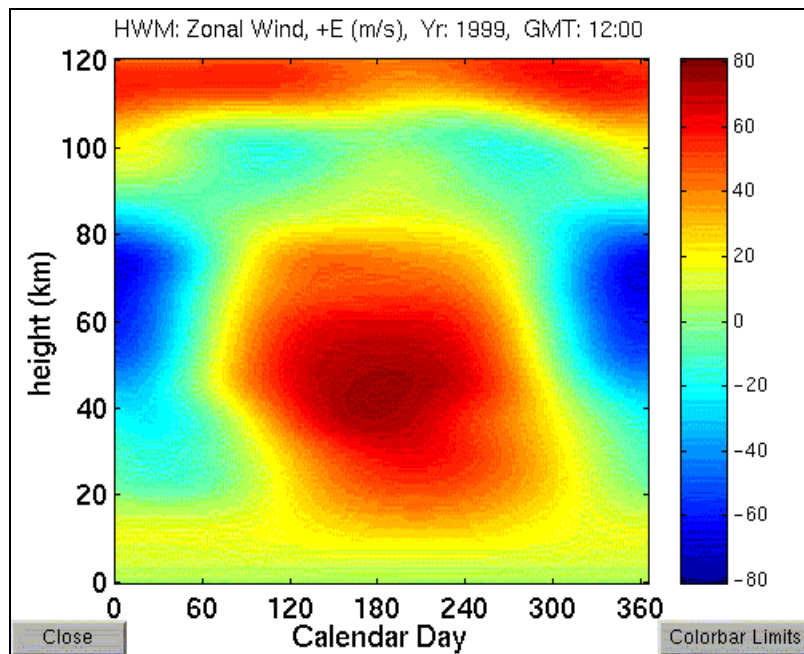


Figure 26. Zonal winds (+Eastward) at South Pacific source location over annual cycle.

4.8.2 Signal Velocity.

Values of signal velocity are shown as a function of source-to-receiver azimuth in Figures 27 and 28. Figure 27 is for Day 1, and Figure 28 is for Day 182. Most of the rays had turning points in the thermosphere; those rays with turning points in the stratosphere are specified in the figures.

On Day 1, with westward winds, paths with azimuths between 0° and 180° represent upwind propagation, while paths with azimuths between 180° and 360° represent downwind propagation. Figure 27 shows that the upwind paths have lower signal velocities than the downwind paths. Stratospheric rays, denoted by the symbols enclosed by the box, are only predicted in cases of downwind propagation.

On Day 182, with eastward winds, paths with azimuths between 0° and 180° represent downwind propagation, while paths with azimuths between 180° and 360° represent upwind propagation. Figure 28 shows again that the upwind paths have lower signal velocities than the downwind paths and that stratospheric rays, denoted by the symbols enclosed by the box, are only predicted in cases of downwind propagation. The signal velocity varies from approximately 0.19 to 0.32 km/sec.

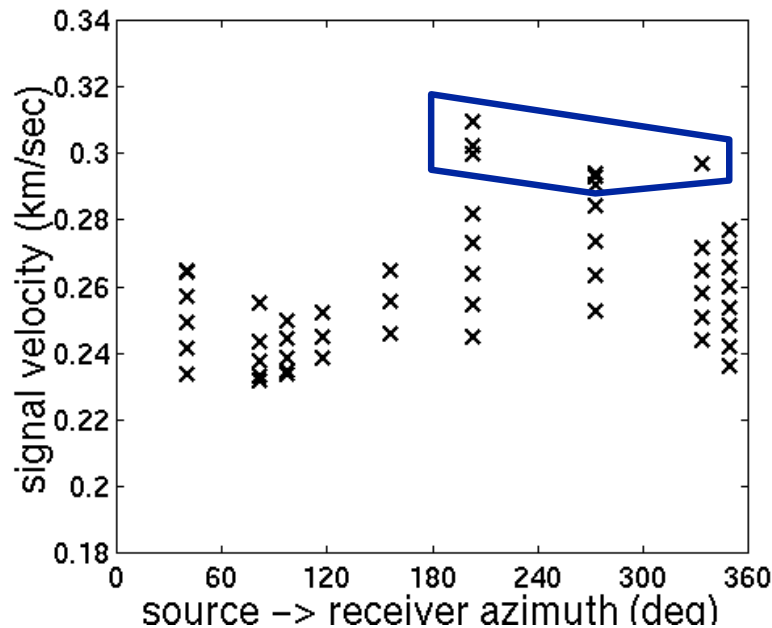


Figure 27. Signal velocities to 9 IMS stations at a range of azimuths; Day 1.

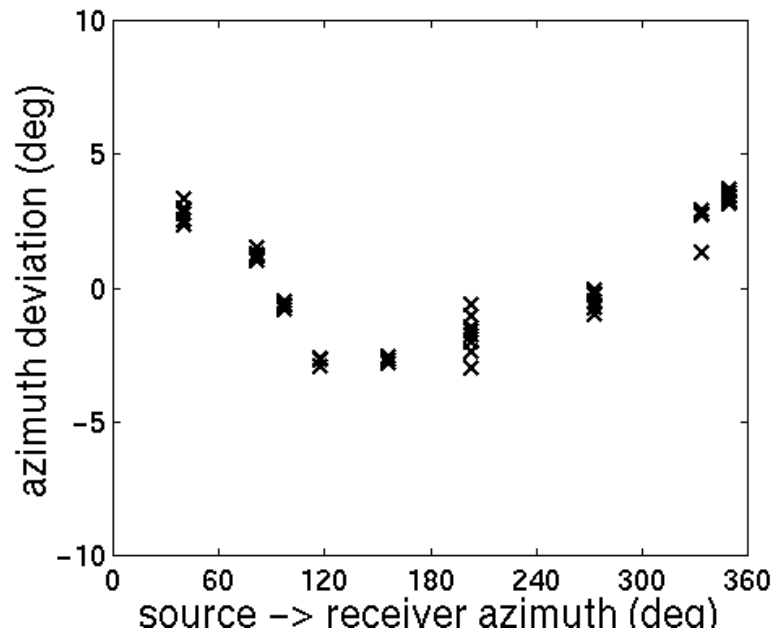


Figure 29. Azimuth deviations to 9 IMS stations at a range of azimuths; Day 1.

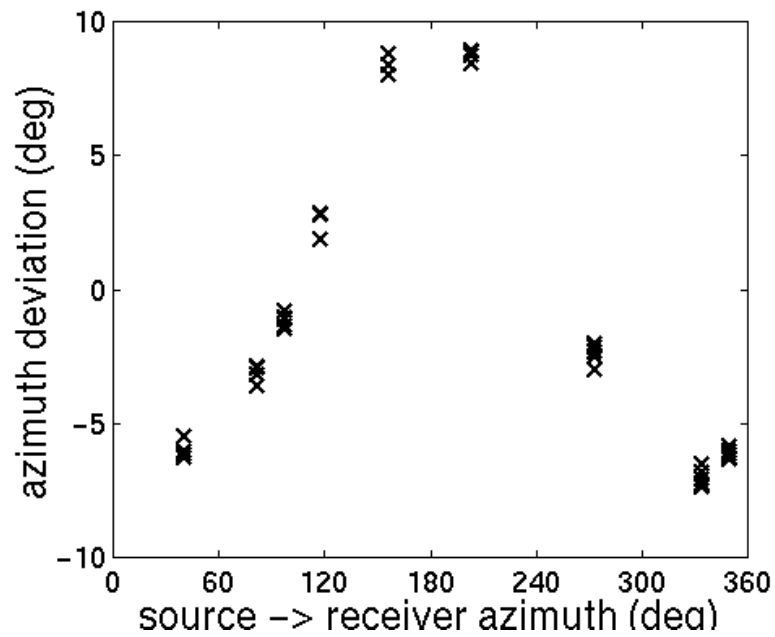


Figure 30. Azimuth deviations to 9 IMS stations at a range of azimuths: Day 182.

4.8.4 Summary of Predicted Biases.

Results are summarized from the study of propagation at various source-to-receiver azimuths (or bearings). The following conclusions are drawn regarding biases in the key parameters that affect source localization. In the presence of strong zonal wind:

- Azimuth deviation depends strongly on bearing;
- The largest values of azimuth deviation are predicted for meridional paths;
- Signal velocity of thermospheric rays varies widely depending on bearing;

The largest deviations from the mean signal velocity are predicted for eastward or westward paths.

4.8.5 Effect of Biases on Localization.

Arrival azimuths observed by infrasound arrays are used in source localization techniques. An operational approach is to look back from each array or station along the observed azimuth. The scenario discussed above is used to study the effect of the predicted biases on source location.

Results from the ray tracing model were used to predict the observed arrival azimuth at each station. This observed azimuth is equal to the sum of the great circle azimuth and the modeled azimuth deviation. Looking back from the stations along the observed azimuths that are predicted using this technique gives an estimate of the source location that might be predicted operationally for this scenario.

There is some uncertainty associated with each estimate of observed arrival azimuth. Referring to Figures 29 and 30, a distribution of azimuth deviation values is shown for each path. The extremes of the distribution at each station are used in this study to identify two azimuths that define bounds of the back-azimuth estimate from that station.

Figures 31 and 32 show, for Day 1 and Day 182, respectively, the intersections that result from looking back on a great circle along the two bounding azimuths from each of the nine stations. The star at the origin of each figure indicates the actual source location used in the modeling. Contours are drawn at 100 km increments. A dot at the end of a back-azimuth indicates a point that is at a range equal to 115% of the known source-to-receiver range.

On Day 1, with westward winds, the back-azimuth intersections are to the west of the actual source. On Day 182, with eastward winds, the back-azimuth intersections, which represent estimates of the source location, are to the east of the actual source. The points of intersection, which represent estimates of the source location, miss the true source location by approximately 100 to approximately 800 km, respectively.

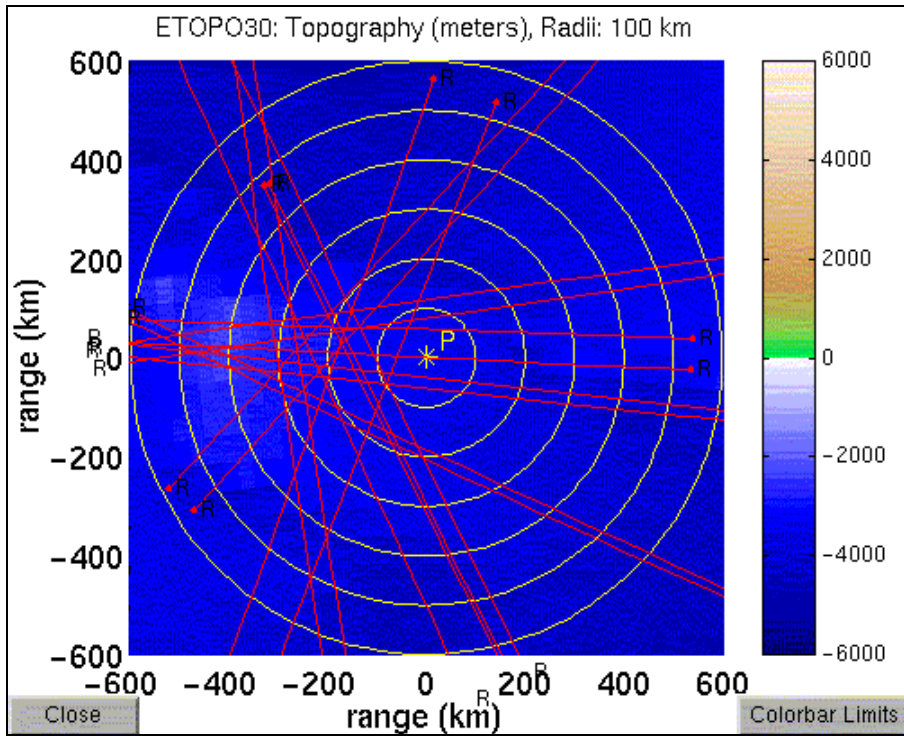


Figure 31. Back-azimuths from 9 IMS stations, with contours at 100 km increments; Day 1.

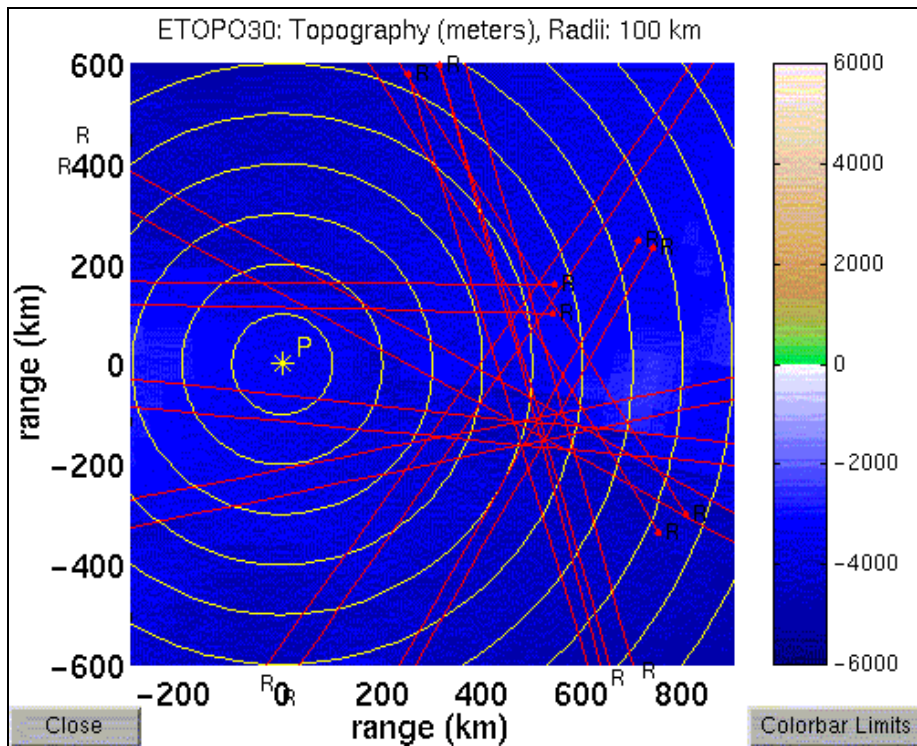


Figure 32. Back-azimuths from 9 IMS stations, with contours at 100 km increments; Day 182.

It should be noted that this could be considered a worst case scenario due to the long paths from the chosen source location and the high zonal winds on the chosen days of the study. Smaller location biases would be anticipated for shorter paths and/or lower wind speeds.

This study shows that the day of year is an important parameter in determining the effect of wind on infrasound propagation. Furthermore, it demonstrates that winds can have a dramatic effect on the accuracy of source localization. The study also indicates that models can be used to determine appropriate corrections to observed arrival azimuths. These corrections could be applied in localization techniques to improve estimates. Large localization errors may occur if corrections are not made for biases in azimuth.

Section 5

Conclusions and Recommendations

A user-friendly software tool kit has been developed to predict the critical propagation characteristics that affect localization and detection performance of an infrasound monitoring network. Travel time, azimuth, and amplitude of atmospheric infrasound phases can be modeled for combinations of source and receiver locations worldwide. The software incorporates a common user interface for:

- Accessing atmospheric characterizations, e.g., temperature and wind profiles,
- Exercising infrasound propagation models,
- Integrating the propagation models with the atmospheric environment, and
- Viewing output data.

The user interface automates many of the procedures necessary for propagation modeling and therefore will lead to increased efficiency among CTBT infrasound researchers and analysts. The tool kit's capabilities can be leveraged in future efforts to generate components of an infrasound knowledge database for use in CTBT monitoring.

The integrated set of models allows for higher fidelity propagation modeling than has previously been available to the infrasound monitoring community. Specific features of the software that represent improvements over existing infrasound modeling capabilities include:

- Integration of range-dependent sound speed and winds with propagation models,
- The ability to account for time-of-day and day-of-year effects rather than simple seasonal or monthly averages,
- An algorithm to identify eigenrays, rays that connect a source and receiver,
- Automatic identification of dual-duct propagation environments and automatic calculation of the summed modal solution for both ducts,
- Development of a perturbation approach to model propagation variability.

The ability to model infrasound propagation and assess source location is therefore enhanced. Further investigations of environmental variability and its effect on propagation should be conducted. Additional development of network performance models incorporating these variability effects should also be performed.

Classes of propagation modeling techniques were reviewed, and ray tracing, normal mode and parabolic equation models were selected as being most appropriate for application to monitoring issues. Model-to-model comparisons should be conducted to validate the modeling techniques and to define confidence levels. Enhancements to the functionality and efficiency of the baseline models should be incorporated into a next-generation version of the software.

Atmospheric databases and models were reviewed, and empirical models of wind and temperature were selected as appropriate characterizations of the propagation environment that could be efficiently integrated with the propagation models. As higher fidelity characterizations become available, they should be integrated into a next-generation version of the software. Efforts should also be made to incorporate near-real-time updates to the propagation environment, based on updated measurements or synoptic models, and to evaluate resulting improvements over the mean environmental models.

Model output has been compared to measured infrasound data corresponding to historical events. Agreement is generally good for a number of cases investigated; however, certain cases are not well modeled using the mean atmospheric characterizations. Additional comparisons with data should be made; these investigations will serve to highlight the areas where further model development is most needed.

Systematic sensitivity analyses have been conducted to understand the effect of temporal, spatial and environmental parameters on accurate modeling of long range infrasound propagation. Major effects on propagation were shown to result from variations in time-of-year, in propagation direction with respect to zonal winds, and in source or receiver latitude. Significant effects on propagation were also predicted due to the diurnal cycle. Smaller variations were predicted due to changes in solar disturbance activity. These sensitivity investigations should continue in order to identify specific areas where additional infrasound research and further development of modeling capabilities are needed.

It has been shown via modeling that significant biases in travel time and azimuth over ranges of CTBT interest are anticipated, and that these biases must be corrected for in order to avoid large location errors. The software tool kit provides the infrastructure for incorporation of a localization capability as well as the existing propagation and variability modeling capabilities. The tool could be upgraded to aid analysts in the operational monitoring community via the addition of infrasound localization and detection algorithms, and through automated linkages to sources of updated atmospheric characterizations and measured infrasound data.

Section 6

References

Armstrong, W.T., 1998: Comparison of infrasound correlation over differing array baselines. Los Alamos National Laboratory Report LA-UR-98-2742, *Proceedings of the 20th Annual Seismic Research Symposium*, Santa Fe New Mex. (UNCLASSIFIED)

Clauter, D. A. and R. R. Blandford, 1996: Capability modeling of the proposed International Monitoring System 60-station infrasonic network, *Fall Meeting of the American Geophysical Union*, San Francisco, Ca. (UNCLASSIFIED)

Dighe, K. A., R. W. Whitaker, and W. T. Armstrong, 1998: Modeling study of infrasonic detection of a 1 kT atmospheric blast, *Proceedings of the 20th Annual Seismic Research Symposium*, Santa Fe, New Mex. (UNCLASSIFIED)

Farrell, T. and K. LePage, 1996: *Development of a Comprehensive Hydroacoustic Coverage Assessment Model*, Air Force Phillips Laboratory Technical Report PL-TR-96-2248, BBN Technical Report No. W1275, Arlington, Va. (UNCLASSIFIED)

Gibson, R., 1998: Integration of atmospheric databases and infrasound propagation models, *Proceedings of the Informal Workshop on Infrasonics*, Bruyeres-le-Chatel, France. (UNCLASSIFIED)

Gibson, R and T. Farrell, 1998: Integration of atmospheric databases and infrasound propagation models, *Proceedings of the 20th Annual Seismic Research Symposium*, Santa Fe, New Mex. (UNCLASSIFIED)

Gibson, R., R. Bieri, and T. Farrell, 1998: *Application of Three-Dimensional Ray Tracing to Infrasonic Propagation in the Atmosphere: The October 1997 El Paso Bolide*, BBN Technical Memorandum No. W1332, Arlington, Va. (UNCLASSIFIED)

Gibson, R., D. Norris, and T. Farrell, 1999: Development and application of an integrated infrasound propagation modeling tool kit, *Proceedings of the 21st Annual Seismic Research Symposium*, Las Vegas, NV. (UNCLASSIFIED)

Hedin, A. E, E. L. Fleming, A. H. Manson, F. J. Schmidlin, S. K. Avery, R. R. Clark, S. J. Franke, G. J. Fraser, T. Tsuda, F. Vial, and R. A. Vincent, 1996: Empirical wind model for the upper, middle, and lower atmosphere, *J. Atmos. Terr. Phys.*, **58**, 1421-1447. (UNCLASSIFIED)

Herrin, E., J. Bonner, P. Golden, C. Hayward, G. Sorrells, J. Swanson, and I. Tibuleac, 1998: Reducing false alarms with seismo-acoustic synergy. *Proceedings of the 20th Annual Seismic Research Symposium*, Santa Fe, New Mex. (UNCLASSIFIED)

- Hunter, J. H. and R. W. Whitaker, 1997: Numerical modeling of long range infrasonic propagation, *Infrasound Workshop for CTBT monitoring*, Santa Fe, New Mex. (UNCLASSIFIED)
- Jensen, F. B., W. A. Kuperman, M. B. Porter, and H. Schmidt, 1994: *Computational Ocean Acoustics*, AIP Press, New York. (UNCLASSIFIED)
- Jones, M. J., J. P. Riley, and T. M. Georges, 1986: *A Versatile Three-Dimensional Hamiltonian Ray-Tracing Program for Acoustic Waves in the Atmosphere above Irregular Terrain*, NOAA Special Report, Wave Propagation Laboratory, Boulder, Co. (UNCLASSIFIED)
- Norris, D. E. and R. Gibson, 1999: Diurnal variability and its effect on ray paths, *Spring Meeting of the American Geophysical Union*, Boston, Mass. (UNCLASSIFIED)
- Norris, D. E. and R. Gibson, 1999: Seasonal variability and its effect on ray paths, *J. Acoust. Soc. Am.*, **106**, No. 4, Pt. 2, 2144. (UNCLASSIFIED)
- Norris, D., R. Nadel, and R. Gibson, 1999: *User's Guide for InfraMAP (Infrasonic Modeling of Atmospheric Propagation)*, BBN Technical Memorandum No. W1353, Arlington, Va. (UNCLASSIFIED)
- Picone, J. M., A. E. Hedin, S. L. Coffey, J. Lean, D. P. Drob, H. Neal, D. J. Melendez-Alvira, R. R. Meier, and J. T. Mariska, 1997: The Naval Research Laboratory program on empirical models of the neutral upper atmosphere, in *Astrodynamics: Advances in the Astronautical Sciences*, Vol. 97, edited by F. R. Hoots, B. Kaufman, P. J. Cefola, and D. B. Spencer, American Astronautical Society, San Diego, Ca. (UNCLASSIFIED)
- Peitgen, H. and D. Saupe, eds., 1998: *The Science of Fractal Images*, Springer-Verlag. (UNCLASSIFIED)
- Pierce, A. D. and J. W. Posey, 1970: *Theoretical Prediction of Acoustic-Gravity Pressure Waveforms Generated by Large Explosions in the Atmosphere*, Technical Report AFCRL-70-0134, Air Force Cambridge Research Laboratories, Bedford, Mass. (UNCLASSIFIED)
- Pierce, A. D., C. A. Moo, and J. W. Posey, 1973: *Generation and Propagation of Infrasonic Waves*, Technical Report AFCRL-TR-73-0135, Air Force Cambridge Research Laboratories, Bedford, Mass. (UNCLASSIFIED)
- Pierce, A. D. and W. A. Kinney, 1976: *Computational Techniques for the Study of Infrasound Propagation in the Atmosphere*, Technical Report AFGL-TR-76-56, Air Force Geophysics Laboratories, Hanscom AFB, Mass. (UNCLASSIFIED)
- ReVelle, D.O., R.W. Whitaker, and W.T. Armstrong, 1998: Infrasound from the El Paso Super-Bolide of October 9, 1997. Los Alamos National Laboratory Report LA-UR-98-2893, in *Characteristics and Consequences of Space Debris and Near-Earth Objects*, SPIE. (UNCLASSIFIED)

West, M., K. E. Gilbert, and R. A. Sack, 1992: A tutorial on the Parabolic Equation (PE) model used for long range sound propagation in the atmosphere, *Applied Acoustics*, **37**, 31-49.
(UNCLASSIFIED)

Appendix

Abbreviations and Acronyms

AFTAC	Air Force Technical Applications Center
AGU	American Geophysical Union
A_p	planetary equivalent disturbance amplitude
AU	Astronomical Unit
CTBT	Comprehensive Nuclear Test Ban Treaty
ETOPO	Earth Topography
FFP	Fast Field Program
FNMOCC	Fleet Numerical Meteorology and Oceanography Command
GUI	Graphical User Interface
HARPA	Hamiltonian Ray-Tracing Program for Acoustic Waves in the Atmosphere
HWM	Horizontal Wind Model
HydroCAM	Hydroacoustic Coverage Assessment Model
IDC	International Data Center
IMS	International Monitoring System
InfraMAP	Infrasonic Modeling of Atmospheric Propagation
LANL	Los Alamos National Laboratory
MSIS or MSISE	Extended Mass Spectrometer - Incoherent Scatter Radar model
NASA	National Aeronautics and Space Administration
NCDC	National Climatic Data Center
NGDC	National Geophysical Data Center
NOAA	National Oceanographic and Atmospheric Administration
NOGAPS	Naval Operational Global Atmospheric Prediction System
NRL	Naval Research Laboratory
PE	Parabolic Equation
PSD	Power Spectral Density
TXIAR	Texas Infrasound Array
UT	Universal Time
WKB	Wentzel-Kramer-Brillouin method

Distribution List

DEPARTMENT OF DEFENSE

DIRECTOR
DEFENSE RESEARCH &
ENGINEERING
WASHINGTON, DC 20301-3110
ATTN: DDR&E

DEFENSE TECHNICAL INFORMATION
CENTER
8725 JOHN J. KINGMAN ROAD, SUITE
0944
FORT BELVOIR, VA 22060-6218
ATTN: DTIC/OCP

DEFENSE THREAT REDUCTION
AGENCY
45045 AVIATION DRIVE
DULLES, VA 20166-7517
ATTN: TDCN, DR A. DAINTY
ATTN: TDS, DR C. GALLAWAY

DEFENSE THREAT REDUCTION
AGENCY
6801 TELEGRAPH ROAD
ALEXANDRIA, VA 22310-3398
ATTN: CTR, L. KLUCHKO
ATTN: TD, DR D. LINGER
ATTN: TDANP, TRC
ATTN: TDC, M. SHORE
ATTN: TDCN, R. JIH

HEADQUARTERS
DEFENSE THREAT REDUCTION
AGENCY
8725 JOHN J. KINGMAN ROAD, MS-
6201
FT BELVOIR, VA 22060-6201
ATTN: TDCS, DR J. FOX

DEFENSE THREAT REDUCTION
AGENCY
ALBUQUERQUE OPERATIONS
1680 TEXAS STREET, SE
KIRTLAND AFB, NM 87117-5669
ATTN: TDT-D, DR G. BALADI
ATTN: TDTP, DR B. RISTVET

DEPARTMENT OF DEFENSE CONTRACTORS

ACIS
6T11 NHB
WASHINGTON, DC 20505
ATTN: DR J. FILSON
ATTN: L. TURNBULL
ATTN: T. MURPHY

BATTELLE MEMORIAL INSTITUTE
MUNITIONS & ORDNANCE CTR
505 KING AVENUE
COLUMBUS, OH 43201-2693
ATTN: TACTEC

BBN CORPORATION
1300 N. 17TH STREET, SUITE 1200
ARLINGTON, VA 22209
ATTN: H. FARRELL
ATTN: J. PULLI

BDM CORPORATION OF SAUDI
ARABIA
12150 EAST MONUMENT DRIVE, SUITE
501
FAIRFAX, VA 22033-4050
ATTN: J. STOCKTON, JB 4C22

CALIFORNIA, UNIVERSITY AT SAN
DIEGO
SCRIPPS INSTITUTION OF
OCEANOGRAPHY
P. O. BOX 6049
SAN DIEGO, CA 92166-6049
ATTN: C. DEGROOT-HEDLIN
ATTN: DR M. A. H. HEDLIN
ATTN: PROF F. VERNON
ATTN: PROF J. A. ORCUTT
ATTN: PROF J. BERGER

CENTER FOR MONITORING
RESEARCH
1300 N, 17TH STREET, SUITE 1450
ARLINGTON, VA 22209
ATTN: DR K. L. MCLAUGHLIN
ATTN: DR R. NORTH
ATTN: LIBRARIAN
ATTN: R. A. GUSTAFSON
ATTN: V. RYABOY

CTB TREATY MANAGER
ROSSLYN GATEWAY
1901 N. MOORE STREET, SUITE 609
ARLINGTON, VA 22209
ATTN: DR R. W. ALEWINE, III

DGI
3612 SURFWOOD RD
MALIBU, CA 90265
ATTN: R. F. HERBST

ENSCO, INC
445 PINEDA COURT
MELBOURNE, FL 3940
ATTN: DR D. TAYLOR

ENSCO, INC.
P. O. BOX 1346
SPRINGFIELD, VA 22151-0346
ATTN: D. BAUMGARDT
ATTN: Z. DER

**DEPARTMENT OF DEFENSE
CONTRACTORS**
GEOPHEX, LTD.
WESTON GEOPHYSICAL
325 WEST MAIN STREET
NORTHBOROUGH, MA 01532
ATTN: DR D. REITER
ATTN: MR J. LEWKOWICZ

ITT INDUSTRIES
ITT SYSTEMS CORPORATION
ATTN: AODTRA/DTRIAC
1680 TEXAS STREET, SE
KIRTLAND AFB, NM 87117-5669
ATTN: DTRIAC
ATTN: DTRIAC/DARE

JAYCOR
1410 SPRING HILL ROAD, SUITE 300
MCLEAN, VA 22102
ATTN: DR C. P. KNOWLES
ATTN: T. J. HANNIGAN

JAYCOR, INC.
P. O. BOX 85154
SAN DIEGO, CA 92138-5154
ATTN: M. TREADAWAY
ATTN: R. STAHL

LACHEL & ASSOCIATES INC.
P. O. BOX 5266
GOLDEN CO 80401
ATTN: D. LACHEL

LOGICON INC.
LOGICON ADVANCED TECHNOLOGY
2100 WASHINGTON BLVD
ARLINGTON, VA 22204-5704
ATTN: F. DICKERSON

LOGICON R AND D ASSOCIATES
P. O. BOX 100
PAHRUMP, NV 89041
ATTN: J. LACOMB

MAXWELL LABORATORIES, INC.
S-CUBED WASHINGTON RESEARCH
OFFICE
11800 SUNRISE VALLEY DRIVE, SUITE
1212
RESTON, VA 22091
ATTN: DR. T. J. BENNETT
ATTN: J. R. MURPHY

MAXWELL TECHNOLOGIES INC.
SYSTEMS DIVISION
9210 SKY PARK COURT
SAN DIEGO, CA 92123-4302
ATTN: DR E. PETERSON
ATTN: DR J. L. STEVENS
ATTN: DR G. E. BAKER

MISSION RESEARCH CORP.
8560 CINDERBED ROAD, SUITE 700
NEWINGTON, VA 22122
ATTN: DR. M. FISK

MULTIMAX, INC
1441 MC CORMICK DRIVE
LANDOVER, MD 20785
ATTN: DR I. N. GUPTA
ATTN: DR W. CHAN
ATTN: MS L. GRANT

PACIFIC NORTHWEST LABORATORIES
A DIV OF BATTELLE MEMORIAL INST.
P. O. BOX 999
RICHLAND, MA 99352
ATTN: TECHNICAL STAFF, MS
K5-12

PACIFIC-SIERRA RESEARCH CORP.
WASHINGTON OPERATIONS
1400 KEY BOULEVARD, SUITE 700
ARLINGTON, VA 22209
ATTN: N. L. DUNCAN

S-CUBED
A DIVISION OF MAXWELL LABS, INC.
11800 SUNRISE VALLEY DRIVE, SUITE
1212
RESTON, VA 22091
ATTN: J. MURPHY

SCIENCE & ENGINEERING
ASSOCIATES, INC.
7918 JONES BRANCH DRIVE, SUITE
500
MCLEAN, VA 22102
ATTN: R. BEATY

SCIENCE APPLICATION INT'L CORP.
3309 NW GOLDEN PLACE
SEATTLE, WA 98117
ATTN: A. RATLETON

SCIENCE APPLICATIONS INTL CORP.
10260 CAMPUS POINT DRIVE
SAN DIEGO, CA 92121-1578
ATTN: DR T. C. BACHE, JR.
ATTN: DR T. J. SERENO, JR.

SCIENCE APPLICATIONS INTL CORP
2111 EISENHOWER AVENUE, SUITE
205
ALEXANDRIA, VA 22314
ATTN: DR D. PIEPENBURG

SCIENCE APPLICATIONS INTL CORP.
GEOSPATIAL DATA DEVELOPMENT
DIVISION
700 SOUTH BABCOCK STREET, SUITE
300
MELBOURNE, FL 32901
ATTN: R. BJURSTROM

SCIENCE APPLICATIONS INTL CORP.
P. O. BOX 1303
MCLEAN, VA 22102
ATTN: D. BACON

SOUTHERN METHODIST UNIVERSITY
DEPT OF GEOLOGICAL SCIENCE
P. O. BOX 395
DALLAS, TX 75275-0395
ATTN: DR B. STUMP
ATTN: E. HERRIN

SRI INTERNATIONAL
333 RAVENSWOOD AVENUE
MENLO PARK, CA 94025-3434
ATTN: D. CURRAN

ST LOUIS UNIVERSITY
P. O. BOX 8148
PIERRE LACLEDE STATION
ST LOUIS, MO 63156-8148
ATTN: PROF B. HERRMANN
ATTN: PROF B. J. MITCHELL

TASC, INC
1101 WILSON BOULEVARD, SUITE
1500
ARLINGTON, VA 22209-2248
ATTN: J. A. MOSORA

TEXAS, UNIVERSITY AT AUSTIN
P. O. BOX 7726
AUSTIN, TX 78712
ATTN: C. A. FROELICH

WOODWARD-CLYDE CONSULTANTS
566 EL DORADO STREET
PASADENA, CA 91109-3245
ATTN: DR B. B. WOODS
ATTN: DR C. K. SAIKIA

DEPARTMENT OF ENERGY

BECHTEL NEVADA
P. O. BOX 809
LOS ALAMOS, NM 87544-0809
ATTN: D. EILERS

BECHTEL NEVADA, INC
P. O. BOX 98521
LAS VEGAS, NV 89193-8521
ATTN: D. BARKER, M/S NLV053

DEPARTMENT OF ENERGY
1000 INDEPENDENCE AVENUE SW
WASHINGTON, DC 20585
ATTN: D. WATKINS, NN-42/GA007
ATTN: E. MANAK, NN-30/FORS
ATTN: E. STOVER
ATTN: S. RUDNICK/NN-20

UNIVERSITY OF CALIFORNIA
LAWRENCE LIVERMORE NATIONAL
LAB
P. O. BOX 808
LIVERMORE, CA 94551-9900
ATTN: K. NAKANISHI
ATTN: W. J. HANNON, JR, MS, L-103
ATTN: F. HEUZE, MS, L-200
ATTN: L. GLENN, MS, L-200
ATTN: DR J. ZUCCA, MS, L-205
ATTN: M. DENNY, MS, L-205
ATTN: TECHNICAL STAFF, MS, L-200
ATTN: TECHNICAL STAFF, MS, L-208
ATTN: TECHNICAL STAFF, MS, L-205

LOS ALAMOS NATIONAL
LABORATORY
P. O. BOX 1663
MAIL STOP G-733
LOS ALAMOS, NM 87545
ATTN: F. CHAVEZ, MS-D460
ATTN: D. WESTERVELT, MS-A112
ATTN: D. STEEDMAN, MS-F607
ATTN: TECHNICAL STAFF, MS-C335
ATTN: TECHNICAL STAFF, MS-D460
ATTN: TECHNICAL STAFF, MS-F665

PACIFIC NORTHWEST NATIONAL
LABORATORY
P. O. BOX 999
BATTELLE BOULEVARD
RICHLAND, WA 99352
ATTN: D. N. HAGEDORN, MS K5-12

SANDIA NATIONAL LABORATORIES
ATTN: MAIL SERVICES
P. O. BOX 5800
ALBUQUERQUE, NM 87185-0459
ATTN: TECHNICAL STAFF, DEPT
5704, MS 0655
ATTN: TECHNICAL STAFF, DEPT
5704, MS 0979
ATTN: TECHNICAL STAFF, DEPT
5736, MS 0655
ATTN: TECHNICAL STAFF, DEPT
9311, MS 1159

SEISMOLOGICAL LABORATORY 252-21
CALIFORNIA INSTITUTE OF
TECHNOLOGY
PASADENA, CA 91125
ATTN: T. AHERNS

UNIVERSITY OF CALIFORNIA
EARTH SCIENCE DIVISION
479 MCCONE HALL, LBNL, 90-2106
BERKELEY, CA 94720
ATTN: L. JOHNSON, MS-90-1116

DEPARTMENT OF THE AIR FORCE

HEADQUARTERS
AFTAC/TTR
1030 SOUTH HIGHWAY A1A
PATRICK AFB, FL 32925-3002
ATTN: V. HSU

AIR FORCE RESEARCH LABATORY
29 RANDOLPH ROAD
HANSCOM AFB, MA 01731-5000
ATTN: DR D. HARKRIDER
ATTN: DR D. REITER
ATTN: GPE, J. LEWKOWICZ
ATTN: J. RONG-SONG

AIR FORCE RESEARCH LABORATORY
5 WRIGHT STREET
HANSCOM AFB, MA 01731-3004
ATTN: RESEARCH LIBRARY, TL

AIR FORCE TECH APPLICATIONS
CENTER
1300 17TH STREET, SUITE 1450
ARLINGTON, VA 22209
ATTN: R. BLANDFORD

AIR FORCE TECHNICAL
APPLICATIONS CTR/TT
1030 S HIGHWAY AIA
PATRICK AFB, FL 32925-3002
ATTN: CA/STINFO
ATTN: DR B. KEMERAIT
ATTN: DR D. RUSSELL
ATTN: G. ROTHE, TTR
ATTN: J. C. LUCAS
ATTN: M. SIBOL

DIRECTORY OF OTHER (LIBRARIES AND UNIVERSITIES)

ARIZONA, UNIVERSITY OF
DEPT. OF GEOSCIENCES/SASO
TUCSON, AZ 85721
ATTN: PROF T. C. WALLACE

BOISE STATE UNIVERSITY
GEOSCIENCES DEPARTMENT
1910 UNIVERSITY DRIVE
BOISE, ID 83725
ATTN: J. E. ZOLLWEG

BOSTON COLLEGE
INSTITUTE FOR SPACE RESEARCH
140 COMMONWEALTH AVENUE
CHESTNUT HILL, MA 02167
ATTN: PROF L. SYKES

CALIFORNIA INSTITUTE OF
TECHNOLOGY
DIVISION OF GEOLOGY & PLANETARY
SCIENCES
PASADENA, CA 91125
ATTN: PROF D. V. HELMBERGER

CALIFORNIA-DAVIS, UNIVERSITY OF
DAVIS, CA 95616
ATTN: R. H. SHUMWAY, DIV
STATISTICS
ATTN: S. E. KIM

CALIFORNIA-SANTA CRUZ,
UNIVERSITY OF
INSTITUTE OF TECTONICS
SANTA CRUZ, CA 95064
ATTN: DR R. S. WU
ATTN: PRO T. LAY

COLORADO-BOULDER, UNIVERSITY
OF
BOULDER, CO 80309
ATTN: M. RITZWOLLER,
CAMPUS BOX 390
ATTN: PROF C. ARCHAMBEAU

COLUMBIA UNIVERSITY
LAMONT-DOHERTY EARTH
OBSERVATORY
PALISADES, NY 10964
ATTN: DR L. R. SYKES
ATTN: DR J. XIE
ATTN: PROF P. G. RICHARDS

CONNECTICUT, UNIVERSITY OF
DEPT. OF GEOLOGY & GEOPHICS
STOORS, CT 06269-2045
ATTN: PROF V. F. CORMIER, U-45,
ROOM 207

CORNELL UNIVERSITY
DEPARTMENT OF GEOLOGICAL
SCIENCES
3126 SNEE HALL
ITHACA, NY 14853
ATTN: PROF M. BARAZANGI

HARVARD UNIVERSITY
HOFFMAN LABORATORY
20 OXFORD STREET
CAMBRIDGE, MA 02138
ATTN: PROF A. DZIEWONSKI
ATTN: PROF G. EKSTROM

IRIS
1200 NEW YORK AVENUE, NW, SUITE
800
WASHINGTON, DC 20005
ATTN: DR D. SIMPSON
ATTN: DR G. E. VAN DER VINK

MASSACHUSETTS INSTITUTE
OF TECHNOLOGY
EARTH RESOURCES LABORATORY
42 CARLETON STREET
CAMBRIDGE, MA 02142
ATTN: PROF M. N. TOKSOZ

MICHIGAN STATE UNIVERSITY
LIBRARY
450 ADMINISTRATION BUILDING
EAST LANSING, MI 48824
ATTN: K. FUJITA

NEW MEXICO STATE UNIVERSITY
DEPARTMENT OF PHYSICS
LAS CRUCES, NM 88003
ATTN: PROF J. NI
ATTN: PROF T. HEARN

PENNSYLVANIA STATE UNIVERSITY
GEOSCIENCES DEPARTMENT
403 DEIKE BUILDING
UNIVERSITY PARK, PA 16802
ATTN: PROF C. A. LANGSTON
ATTN: PROF S. ALEXANDER

SAN DIEGO STATE UNIVERSITY
DEPT OF GEOLOGICAL SCIENCES
SAN DIEGO, CA 92182
ATTN: PROF S. M. DAY

SOUTHERN METHODIST UNIVERSITY
FONDREN LIBRARY
DALLAS, TX 75275
ATTN: B. STUMP
ATTN: G. MCCARTOR, DEPT OF
PHYSICS
ATTN: H. L. GRAY, DEPT OF
STATISTICS

UNIVERSITY OF COLORADO
CAMPUS BOX 583
BOULDER, CO 80309
ATTN: DR A. L. LEVSHIN

UNIVERSITY OF SOUTHERN
CALIFORNIA
520 SEAVER SCIENCE CENTER
UNIVERSITY PARK
LOS ANGELES, CA 90089-0483
ATTN: PROF C. G. SAMMIS

FOREIGN

AUSTRALIAN GEOLOGICAL
SURVEY ORGANIZATION
CORNER OF JERRAGOMRRRA AND
NINDMARSH DRIVE
CANBERRA, ACT 2609
AUSTRALIA
ATTN: D. JEPSON

GEOPHYSICAL INSTITUTE OF ISRAEL
HAMASHBIR STREET, 1
HOLON, 58122 ISRAEL
ATTN: DR Y. GITTERMAN

I.R.I.G.M. - B.P. 68
38402 ST. MARTIN D'HERES
CEDEX, FRANCE
ATTN: DR M. BOUCHON

MINISTRY OF DEFENSE/
PROCUREMENT EXECUTIVE
ALACKNESS, BRIMPTON
READING FG7-4RS ENGLAND
ATTN: DR P. MARSHALL

NTNF/NORSAR
P. O. BOX 51
N-2007 KJELLER, NORWAY
ATTN: DR F. RINGDAL
ATTN: T. KVAERNA

OBSERVATOIRE DE GRENOBLE
I.R.I.G.M. - B.P. 53
38041 GRENOBLE, FRANCE
ATTN: DR M. CAMPILLO

RESEARCH SCHOOL OF EARTH
SCIENCES
INSTITUTE OF ADVANCES STUDIES
G. P. O. BOX 4
CANABERRA 2601, AUSTRALIA
ATTN: PROF B. L. N. KENNETT

RUHR UNIVERSTY/BOCHUM
INSTITUTE FOR GEOPHYSIK
P. O. BOX 102148
463 BOCHUM 1, GERMANY
ATTN: PROF H. P. HARJES

SEISMOLOGICAL DIVISION
IRPG
P.O. BOX 2286
HOLON 58122
ISRAEL
ATTN: A. SHAPIRA

SOCIETE RADIOMANA
27 RU CLAUDE BERNARD
75005 PARIS, FRANCE
ATTN: DR B. MASSINON
ATTN: DR P. MECHLER

UNIVERSITY OF BERGEN
INSTITUTE FOR SOLID EARTH

PHYSICS
ALLEGATION 40
N-5007 BERGEN, NORWAY
ATTN: R. E. HUSEBYE

UNIVERSITY OF CAMBRIDGE
DEPARTMENT OF EARTH SCIENCES
MADINGLEY RISE, MADINGLEY ROAD
CAMBRIDGE CB3 0EZ, ENGLAND
ATTN: PROF K. PRIESTLEY

US DEPARTMENT OF THE INTERIOR
US GEOLOGICAL SURVEY NATIONAL
CENTER
MILITARY GEOLOGY PROJECT
12201 SUNRISE VALLEY DRIVE
RESTON, VA 22029
ATTN: B. LEITH
ATTN: DR J. FILSON
ATTN: W. LEITH, MS 928

OTHER GOVERNMENT

CENTRAL INTELLIGENCE AGENCY
WASHINGTON, DC 20505
ATTN: CHIEF, OTI/MNG/NWTT -
ST47 NHB

NATIONAL ARCHIVES AND
RECORDS ADMINISTRATION
8601 ADELPHI ROAD, ROOM 3360
COLLEGE PARK, MD 20740-6001
ATTN: USER SERVICE BRANCH

NATIONAL PHOTOGRAPHIC
INTERPRETATION CENTER
SOUTHWEST STATION
P. O. BOX 70967
WASHINGTON, D C 20024-0967
ATTN: K. TIGHE-WHITE
ATTN: M. BURNS

U S DEPARTMENT OF STATE
320 21ST STREET, NW
WASHINGTON, DC 20451
ATTN: DR E. LACEY, ACDA/IVI,
ROOM 5741
ATTN: K. WARD
ATTN: R. DAY
ATTN: T. RAY